Iowa State University
Digital Repository

Graduate Theses and Dissertations

Iowa State University Capstones, Theses and Dissertations

2014

Effects of electrical, thermal and thermal gradient stress on reliability of metal interconnects

Srijita Patra
Iowa State University

Follow this and additional works at: https://lib.dr.iastate.edu/etd

Part of the Electrical and Electronics Commons

Recommended Citation
Patra, Srijita, "Effects of electrical, thermal and thermal gradient stress on reliability of metal interconnects" (2014). *Graduate Theses and Dissertations*. 14054.
https://lib.dr.iastate.edu/etd/14054

This Thesis is brought to you for free and open access by the Iowa State University Capstones, Theses and Dissertations at Iowa State University Digital Repository. It has been accepted for inclusion in Graduate Theses and Dissertations by an authorized administrator of Iowa State University Digital Repository. For more information, please contact digirep@iastate.edu.

المنارة للاستشارات

www.manaraa.com

Effects of electrical, thermal and thermal gradient stress on reliability of metal interconnects

by

Srijita Patra

A thesis submitted to the graduate faculty

in partial fulfillment of the requirements for the degree of

MASTER OF SCIENCE

Major: Electrical Engineering

Program of Study Committee:

Randall Geiger, Major Professor
Degang Chen
Sumit Chaudhary

Iowa State University

Ames, Iowa

2014

Copyright © Srijita Patra, 2014. All rights reserved.

المنارة للاستشارات

www.manaraa.com

DEDICATION

To my Strength, Love and Life: My Parents, Grandma, Sister and Husband

المنارة للاستشارات
www.manaraa.com

TABLE OF CONTENTS

LIST OF FIGURES iv

LIST OF TABLES vi

NOMENCLATURE vii

ACKNOWLEDGEMENTS viii

ABSTRACT ix

CHAPTER 1 - INTRODUCTION 1

CHAPTER 2 - RELIEABILITY MODELING OF METAL INTERCONNECT WITH TIME CONSTANT ELECTRICAL AND THERMAL STRESS 4

2.1 Reliability Modeling 5

CHAPTER 3 -RELIEABILITY MODELING OF METAL INTERCONNECTS WITH TIME DEPENDENT ELECTRICAL AND THERMAL STRESS 12

3.1 Conditional Reliability and Conditional MTF 22
3.2 Equivalent Age Stress 24
3.3 Relation Between MTF and FIT 25
3.4 Practical Considerations and Open Issues 27

CHAPTER 4 - RELIEABILITY MODELING OF METAL INTERCONNECT WITH ELECTRICAL, THERMAL AND THERMAL GRADIENT STRESS 29

4.1 Accuracy Requirements for Temperature and Temperature Gradient Sensors 40

CHAPTER 5 – CONCLUSION 42

REFERENCES 44

PUBLICATIONS 46

المنارة للاستشارات
www.manaraa.com

LIST OF FIGURES

Figure 2.1: CDF plots under constant stress ……………………………………………………..9

Figure 2.2 : MTF is decreasing with increasing stress………………………………………..10

Figure 3.1: Modeling of Time dependent Stress………………………………………………..14

Figure 3.2: 1% high stress and 99% low stress duty cycle…………………………...……15

Figure 3.3: 10% high stress and 80 % low stress duty cycle……………………………………16

Figure 3.4: 50% high stress and 50 % low stress duty cycle……………………………………16

Figure 3.5: 80% high stress and 20 % low stress duty cycle……………………………………17

Figure 3.6: CDF vs time when high stress with 1% duty cycle (DC) and
low stress with 99 % DC..19

Figure 3.7: CDF vs time when high stress with 10% DC and low
stress with 90 % DC……………………………………………………………………19

Figure 3.8: CDF vs time when high stress with 50% DC and
low stress with 50 % DC………………………………………………………………20

Figure 3.9: CDF vs time when high stress with 80% DC and
low stress with 20 % DC……………………………………………………………..20

Figure 3.10: CDF vs time when MTF is ±10% of the target MTF,
temperature is within $\pm1.6^0$C……………………………………………………..22

Figure 3.11: Conditional reliability function to measure conditional MTF……………………...23

Figure 3.12 : Relation between MTF and FIT in different values of experiment time……..…..26

Figure 3.13 : Relation between MTF and log (FIT) in different experiment time ……………...27

Figure 4.1 Arrangement to produce thermal gradient ………………………………………...32

Figure 4.2: CDF plots under different ΔT in T_{NOM} and J_{NOM} conditions……………………........34

Figure 4.3: CDF plots under different T and J in absence of ΔT……………………………......35

Figure 4.4: CDF plots under different T, J when $\Delta T = 0.09^0$ C/μm…………………………….......36

المنارة للاستشارات

www.manaraa.com

Figure 4.5: CDF plots under different T,J when $\Delta T = 0.19^0$ C/µm……………………………..37

Figure 4.6: CDF plots under different T,J when $\Delta T = 0.28^0$ C/µm……………………………..38

Figure 4.7: CDF vs time when MTF is ±10% of the target MTF
under fixed current density and temperature measurement
and temperature gradient is within $\pm 0.011^0$C/µm…………………………………..40

المنارة للاستشارات

www.manaraa.com

LIST OF TABLES

Table 2.1 MTF in Different Constant Stress……………………………………………………9

Table 3.1 Different MTF in Time Variant Stress …………………………………….................18

Table 4.1 : Different Temperature Gradient Conditions and corresponding
Time to Failure (TTF) …………………………………………………………….32

Table 4.2 : MTF in Different ΔT with normal Stress…………………………………………...34

Table 4.3 : MTF in Different Stress in absence of ΔT…………………………………………...36

Table 4.4 : MTF in Different Stress when ΔT=0.09^{0} C/μm…………………………………...37

Table 4.5 : MTF in Different Stress when ΔT=0.19^{0} C/μm……………………………………..38

Table 4.6 : MTF in Different Stress when ΔT=0.28^{0} C/μm……………………………………...39

المنارة للاستشارات

www.manaraa.com

NOMENCLATURE

EM	Electromigration
PDF	Probability Density Function
CDF	Cumulative Density Function
MTF	Median Time to Failure
MTTF	Mean Time to Failure
TM	Thermomigration

المنارة للاستشارات
www.manaraa.com

ACKNOWLEDGEMENTS

I would like to take this opportunity to express my gratitude to those who helped me on so many aspects for my research. First of all, I am grateful to Dr. Randall Geiger for his constant guidance and encouragement. I am thankful to SRC for funding this project. Furthermore, I would also like to extend my thanks to other committee members: Dr. Degang Chen, Dr. Sumit Chaudhary for their insightful advices, despite of their busy schedules. I am blessed to have some good friends for their loving guidance and companionship during my study at ISU.

Finally, I would like to dedicate this thesis to my parents, grandma, sister and husband for whom my life is worthwhile.

للاستشارات المنارة
www.manaraa.com

ABSTRACT

This thesis focuses on the reliability modeling of metal interconnects under time-dependent stress. Whereas most existing reliability models are based upon the assumption that stress is constant throughout the useful life of a system, this thesis considers the more general and more realistic situation where the stress is time-dependent. In this work the stress is defined by temperature and current density variables. It is assumed that the Cumulative Density Function (CDF) is characterized by a single stress parameter that incorporates all stress-dependent variables. A closed-form expression that can be used to calculate the CDF under time-varying stress is presented and this can be used to determine the corresponding Median Time to Failure (MTF). A single parameter which can be represented as a real number is used to incorporate the total effects of the stress history making this approach applicable for dynamic power/thermal management algorithms.

A reliability model that includes the effects of thermal gradient stress in the presence of temperature and current stress is also introduced. With these models, temperature measurement accuracy requirements are developed that are necessary if power/thermal management circuits are to be successful in achieving 10% accuracy in the MTF. Incorporation of a time-dependent stress model that incorporates the user-dependent electrical and thermal stress history in the power/thermal management module of a large integrated circuit offers potential for significantly improving system performance while maintaining a target reliability throughout the operating life of the integrated circuit or for improving the reliability when operated at a user-determined stress level.

www.manaraa.com

CHAPTER 1 - INTRODUCTION

Electromigration in integrated circuit metallization is of considerable importance in today's microelectronics industry. This decades-old problem which passes from technology node to technology node is a major contributor to the limited lifetime of integrated circuits and the associated reduction in reliability. It can be attributed to pressure on semiconductor manufacturers to set maximum current density limits at a level that allows designers to minimize the area and parasitic capacitances in metal interconnects. The resultant high current density creates drift in metal atoms that ultimately causes the interconnects to fail due to mass transport of atoms comprising the interconnect. This mass transport is due to momentum transfer between conducting electrons and metal atoms. In extreme situations, electromigration (EM) causes open circuits by creating voids in interconnects or creates short circuits due to hillocks bridging two conductors operating at different voltage levels though an interconnect effectively fails before the extreme open-circuit or short-circuit conditions occur [1].

Many papers have been written on modeling electromigration in interconnects in integrated circuits since the seminal work of Black in 1967 [2] and 1969 [3]. In his work, Black predicted the Mean Time to Failure (or the Median Time to Failure) in interconnects and the mathematical equation that characterizes this statistic is widely referred to as Black's equation. Black's equation which was obtained from experimental results validated by numerical analysis in [4]. Alam and coworkers [5] used the best estimates of material parameters and an analytical model to compare electromigration lifetimes of Al and Cu dual damascene interconnect lines. The line scaling effect on EM reliability was investigated using three different line widths by Pyun [6]. In this work, EM lifetimes were found to be similar with intrinsic failures caused by

www.manaraa.com

void formation in the line trench driven by interfacial mass transport. Also using Black's equation, CDF plots were shown. A generalized bimodal lognormal distribution model was introduced by Filippi [7]. All of the work [8-9] on MTF focused on time independent stress. But the useful life of an integrated circuit depends strongly upon the level of stress that is applied to the device. This stress is usually time and temperature dependent.

In this thesis a reliability model for electromigration-induced failure in metal interconnects under time-dependent stress is introduced. In contrast to existing reliability models that are based upon the assumption that stress is constant throughout the useful life of a system, this model includes provisions for the more realistic situation where both thermal stress and current stress are time-dependent. A single parameter which can be represented as a real number is used to incorporate the total effects of the stress history of a device making this approach applicable for dynamic power/thermal management algorithms.

Electromigration will probabilistically result in failure of interconnects within the useful life of an integrated circuit if the drift rate of metal atoms in the interconneces is too large. Local power dissipation variations, in part attributable to joule heating, produce thermal gradients. Thermal gradients cause degradation in interconnects through thermomigration (TM). Although, the magnitude of TM flux is much smaller than EM flux, thermal gradients in the presence of high current densities significantly degrade the reliability of interconnects [10], [11]. Though many authors express concern about the effects of thermal gradients on the reliability of interconnects, there are limited research results in the literature that focus on the effects of thermal gradients on electromigration. Large currents also cause non uniform joule heating in interconnects which produce thermal gradients on the semiconductor die. These thermal gradients induce thermomigration (TM) which enhances electromigration (EM). The sleep

المنارة للاستشارات

www.manaraa.com

modes of select functional blocks in high performance chips cause significant temperature gradients on the substrate. In [12] it has been reported that thermal variations of 40°C across a die can exist in a high-performance microprocessor design and these large thermal variations cause large thermal gradients. Power reduction techniques such as dynamic power management [13] and clock gating can result in large thermal gradients. With circuits moving toward higher speeds with clock frequencies in the GHz range and beyond, the magnitude of thermal gradients in the substrate are projected to increase further. In addition, as minimum feature sizes shrink further, the topmost metal layers that carry global signals get closer to the substrate [14]. As a result, the effect of the non-uniform substrate temperature on the interconnect thermal profile becomes more critical.

Temperature has an important effect on the circuit performance and reliability [15]. Neglecting thermal gradients in the median time to failure calculation can introduce major errors. An empirical reliability model for electromigration-induced failure in metal interconnects under thermal, electrical, and thermal gradient stress is introduced in this work. Based upon the limited reported measurements on static thermal gradient stress that are available, this model incorporates thermal gradient stress into the probability density function of the failure time, t_F. With this model, temperature measurement accuracy and temperature gradient measurement accuracy requirements for multi-site on-chip sensors that can be used in power/thermal management algorithms are developed.

المنارة للاستشارات

www.manaraa.com

CHAPTER 2 - RELIEABILITY MODELING OF METAL INTERCONNECT WITH TIME CONSTANT ELECTRICAL AND THERMAL STRESS

A reliability model for electromigration-induced failure in metal interconnects under time independent stress is introduced in this chapter[1]. A single time-dependent parameter which can be represented as a real number is used to incorporate the accumulated effects of the stress into the reliability model.

The mean time to failure (MTTF) or the median time to failure (MTF) are often used as metrics to characterize the reliability of an interconnect. Though the intended useful life of a component is often considerably less than the MTTF or MTF, these metrics are widely used characterize reliability. Although most reliability assessments of electronic components are based upon an assumption of constant stress throughout the operating life of a component, stress is invariably highly time-dependent and this time dependence should be included in reliability models if accurate reliability results are to be obtained.

Accelerated-stress lifetime testing is widely used for experimentally measuring reliability in the semiconductor industry. In most of the experiments, accelerated lifetime testing is based on constant stress. Correspondingly, accelerated lifetime testing results are widely used to predict lifetime, e.g. MTF, under a “normal” operating stress which is invariably assumed to be time independent. Unfortunately, the actual stress is seldom time invariant. Because of the highly nonlinear relationship between lifetime and stress, the assumption of time-invariant stress introduces large errors in lifetime predictions. As a consequence, systems are often over-designed to assure acceptable reliability when the stress is time dependent or target reliability goals are not met when stress actually is nearly constant at an upper-stress bound.

---

[1] This work was supported by the National Science Foundation and the Semiconductor Research Corporation

www.manaraa.com

In most previous work, modeling of electromigration focuses on a statistic such as MTF rather than the Probability Density Function (PDF) of the failure time. And even when the PDF is considered, there is not agreement amongst researchers about what PDF should be used to model the lifetime or how system parameters affect the functional form of the pdf. This lack of agreement is due, in part, to differences in the physical characteristics of the interconnects themselves associated with differences in grain sizes and interconnect geometries.

2.1 Reliability Modeling

In Black's work [2], [3], a single analytical expression for the Mean Time to Failure and the Median Time to Failure, both denoted as MTF, was introduced. Black did not appear to distinguish between these two statistics. The distinction between these metrics is often not clear in the follow-on literature either and some authors use the term time-to-failure, TF, as another statistic to presumably characterize the same effects. To avoid possible confusion in this thesis, the abbreviations MTTF will be used to denote Mean Time to Failure and MTF to denote Median Time to Failure. MTF and MTTF are both statistics of the lifetime of an interconnect which is a random variable characterized by a Probability Density Function $f(t_F)$ where t_F denotes the failure time. The failure time t_F denotes the actual failure time of a device and is a random variable. Corresponding to any Probability Density Function (PDF) is the Cumulative Density Function (CDF) , $F(t_F)$, defined by

$$F(t_F) = \int_{t=0}^{t_F} f(t)\,dt \tag{2.1}$$

$F(t_F)$ is a monotone nondecreasing function of t_F that equals 0 at time $t_F=0$ and converges to 1 as $t_F \rightarrow \infty$. Some authors prefer to work with the Reliability Function $R(t_F)$ (alternatively termed the Survival Function) that is defined as

المنارة للاستشارات
www.manaraa.com

$$R(t_F) = 1 - F(t_F) \quad (2.2)$$

Reliability is defined as the ability of a system or component to perform its required functions under stated conditions for a specific period of time.

$R(t_F)$ is a monotone decreasing function

$$R(t_F) = 1, \text{ when } t_F = 0,$$

$$R(t_F) = 0, \text{ when } t_F \Diamond \infty$$

In this work we concentrate on $F(t_F)$ though trivially the $R(t_F)$ results can be obtained from (2.2).

The MTTF statistic is given by the expression

$$MTTF = \int_{t_F=0}^{\infty} t_F f(t_F) dt_F \quad (2.3)$$

and the MTF statistic by the implicit expression

$$0.5 = \int_{t_F=0}^{MTF} f(t_F) dt_F$$

or equivalently by the explicit expression

$$MTF = F^{-1}(0.5) \quad (2.4)$$

To determine the median time to failure, the model that has been used almost exclusively for the past four decades that was introduced by Black in 1967 can be expressed as

$$MTF = A_0 J^{-N} e^{\left(E_a/kT\right)} \quad (2.5)$$

Black's empirical expression for MTF due to electromigration [2] is usually modified slightly and is expressed as

$$MTF = \begin{cases} \infty & J < J_{CRIT} \\ A_0 (J - J_{CRIT})^{-N} e^{(E_a/kT)} & J > J_{CRIT} \end{cases} \quad (2.6)$$

www.manaraa.com

where T is absolute temperature in K, J is the current density, and k is Boltzman's constant. All parameters in this expression are time-independent. In this expression, there are four process/material dependent model parameters, A_0, J_{CRIT}, N, and E_a. A_0 is a material property and geometry dependent constant. J_{CRIT} is the critical current density. J_{CRIT} is around as 1 MA/ cm^2 for aluminum [17]. N is a constant. The typically range of N is between 1 and 3. For aluminum and copper interconnects N=2 [3] is often used. E_a is the activation energy. For aluminum interconnects E_a typically ranges between 0.7 eV and 0.9 eV.

It is assumed that the amount of wear in the interconnect can be characterized by the time-dependent CDF, specifically, $F(t_F)$. Since the MTF satisfies the relationship

$$MTF = F^{-1}(0.5) \tag{2.7}$$

the MTF is determined from the CDF.

In this work, it will be assumed that the stress is time-dependent but for notational convenience it will be assumed that time is represented by a set of contiguous time intervals and that the stress is constant throughout each time interval. These time intervals scan be arbitrarily short if the stress varies rapidly with time or the time intervals can be long if stress remains relatively constant for long periods of time. It will be assumed that the same functional form of the CDF characterizes the failure time in each interval and that in the ith interval, the stress is completely represented by a single "parameter" in that CDF and this "parameter" is the function $A_0 (J_i - J_{CRIT})^{-N} e^{(E_a/kT_i)}$ where J_i, A_0, J_{CRIT}, N, and T_i are constant throughout the ith interval. It will be assumed that the CDF can be expressed using the lognormal distribution as [18]

$$F_{LNi}(t_F, \mu_i, \sigma) = F_{N01}\left(\frac{\ln(t_F) - \mu_i}{\sigma}\right) \tag{2.8}$$

www.manaraa.com

where

$$\mu_i = \ln\left(A_0 \left(J_i - J_{CRIT}\right)^{-N} e^{(E_a/kT_i)}\right) \quad (2.9)$$

and where F_{N01} denotes the CDF of the Normal (0,1) random variable. The parameter σ is a shape parameter of the distribution and ln(x) is the natural logarithm function and the parameter μ_i denotes the stress level in the ith interval. . It is assumed that if the stress is constant throughout the life of the interconnect, the CDF under two different stress conditions has the following property:

$$\text{If} \quad MTF_a > MTF_b \quad \text{then} \quad F_b(t_F) \geq F_a(t_F) \quad \forall\ t_F \geq 0 \quad (2.10)$$

Circuits are often designed to have an acceptable MTF under constant maximum stress at a given current density denoted as J_{MAX} and a given temperature denoted as T_{MAX}. Typical values for J_{MAX} and T_{MAX} for the 0.45 nm technology node are 3 MA/cm^2 [19] and 110 ^{0}C [20]. These stress conditions are often interpreted as guard bands and power/thermal management algorithms are often established to guarantee that these guard band values are not exceeded with the obvious assumption that if operation is maintained constant at the guard band limit, an acceptable MTF will be obtained.

CDF plots for five different constant stress conditions, characterized by the parameter μ, that are close to J_{MAX} and T_{MAX} based upon the lognormal distribution of (2.8) with shape factor σ=0.3 are shown in Figure 2.1. The stress conditions are listed in Table 2.1 along with the corresponding MTF.

المنارة للاستشارات
www.manaraa.com

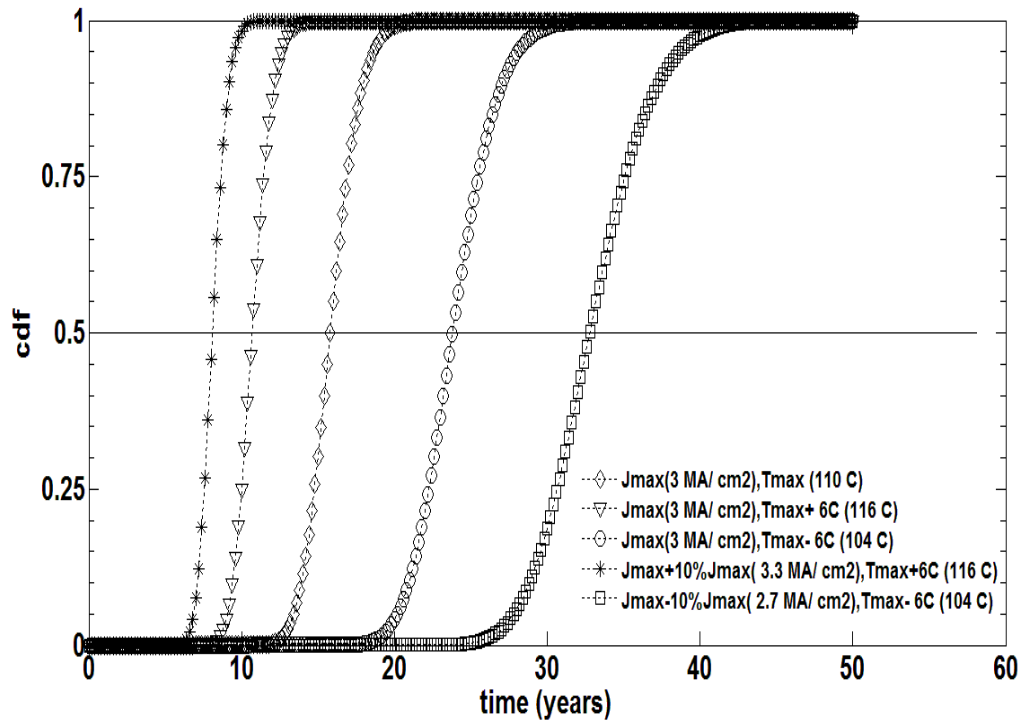

Figure 2.1: CDF plots under constant stress

Table 2.1 MTF in Different Constant Stress

Current Density (J) (MA/cm^2)	**Temperature**	**µ**	**MTF (years)**
3.3(J+10%J)	110^0C+6^0C	2.09	8.1
3	110^0C+6^0C	2.37	10.7
3	110^0C	2.76	15.96
3	110^0C-6^0C	3.17	23.8
2.7 (J-10%J)	110^0C-6^0C	3.50	33

المنارة للاستشارات
www.manaraa.com

A graph is plotted to show the relation between stress and MTF under constant stress in Figure 2.2.

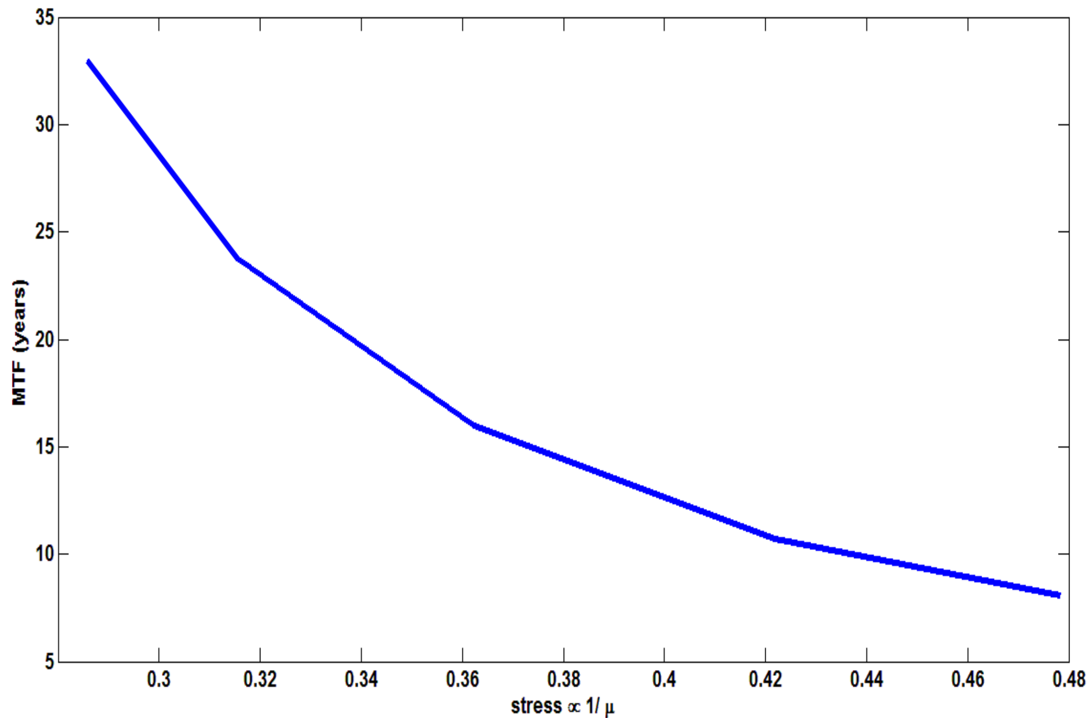

Figure 2.2 : MTF is decreasing with increasing stress

The high sensitivity of the MTF to stress is apparent from these plots. It can be observed that a 10% increment in current density and 6^0C temperature increment causes a 50% reduction in MTF. Even if current stress is unchanged, a 6^0C increment in temperature reduces the MTF by 32%.

Semiconductor manufacturers often give little information about the MTF of their components but internally the reliability of their products is of considerable interest. Since little information is given about the MTF, there is almost no information available about how tightly

المنارة للاستشارات
www.manaraa.com

the MTF is controlled in products but this information should have a significant economic impact on the manufacturer of integrated circuits. Since the MTF is stress dependent, the manufacturers control the MTF by establishing guard bands for temperature and these guard bands are incorporated in the power/thermal management circuitry. But since there will be errors in the temperature sensors that provide input to the power/thermal management unit, these errors will cause a variation in the MTF.

In this work, it will be assumed that the goal of the manufacturer is to maintain an MTF that is within ±10% of the nominal MTF and that temperature sensor accuracy must be established at a level that will keep the MTF within this ±10% window. Following the same approach that was used to obtain Figure 2.1, it can be shown that if the target MTF is 16 years and the current stress is constant at a nominal value of $3MA/cm^2$, the temperature measurement accuracy required to keep the MTF within a ±10% window is $\pm 1.6^0C$. Correspondingly, if the current density also changes by ±5% of the nominal current density, then temperature should be measured with a $\pm 0.5^0C$ accuracy to meet the ±10% MTF window. It should be apparent from these examples that to measure reliability accurately, it is very crucial to precisely monitor the stress profile.

المنارة للاستشارات

www.manaraa.com

CHAPTER 3 -RELIEABILITY MODELING OF METAL INTERCONNECTS WITH TIME DEPENDENT ELECTRICAL AND THERMAL STRESS

In this chapter, a model is developed for the MTF when the electrical and thermal stresses are time variant. For notational convenience, it is assumed that these stresses are piecewise constant and that a sequence of time points, denoted as $\langle t_i \rangle_{i=0}^{m}$, denote times where the stress changes when $m \geq 1$. The time t_0 =0 denotes the "birth" time of the interconnect, that is, the time that a stress is first applied. If the stress remains constant throughout the use of the interconnect, then m=0 and existing models can be used to predict the MTF. When m>0, there are one or more changes in stress. The change in stress at any time point could correspond to a change in J, a change in T, or a change in both J and T. The stress vector ST is defined as

$$ST(t) = \begin{bmatrix} J_0(t) & T_0(t) \\ J_1(t) & T_1(t) \\ \cdots & \\ J_m(t) & T_m(t) \end{bmatrix} \tag{3.1}$$

where

$$\begin{aligned} J_i(t) &= J_i \quad \text{for} \quad t_i \le t < t_{i+1} \quad \forall\, 0 \le i \le m \\ T_i(t) &= T_i \quad \text{for} \quad t_i \le t < t_{i+1} \quad \forall\, 0 \le i \le m \end{aligned} \tag{3.2}$$

and where it is assumed that $t_{m+1} = \infty$ and $J_i > J_{CRIT} \quad \forall i$. These latter two assumptions are made strictly for notational convenience and neither is necessary. It is assumed that in any stress interval, the CDF is equal to that which would be in effect had the same stress been applied at the translated time needed to maintain continuity of the CDF at the transition from the previous interval. This latter assumption is critical in what follows and can be interpreted as assuming that the amount of wear is characterized by the CDF. This wear stress assumption can be expressed mathematically as

المنارة للاستشارات
www.manaraa.com

$$F(t_F) = F_k(t_F) \quad \text{for} \quad t_k < t_F \leq t_{k+1} \quad 0 \leq k \leq m \tag{3.3}$$

where for all $0 \leq k \leq m$,

$$F_k(t_F) = F_{k0}\left(t_F - t_k + F_{k0}^{-1}\left(F_{k-1}(t_k)\right)\right) \quad \text{for} \quad t_k < t_F \leq t_{k+1} \tag{3.4}$$

where $F_k(t_F)$ is the CDF in the interval $t_k < t_F \leq t_{k+1}$ and where $F_{k0}(t_F)$ is the CDF that corresponds to a constant stress of J_k and T_k throughout the life of the interconnect. From this expression, it can be observed that the effects of the entire stress history in any interval $t_k<t_F<t_{k+1}$ is dependent only upon the function $F_{k-1}(t_k)$ and thus only a single real number needs to be stored to predict the reliability at any point in time. This number needs to be updated each time a transition is made to a different interval. It can also be observed that the sequence $\langle F_{k-1}(t_k)\rangle_{k=1}^{\infty}$ is monotone and increasing with k. The pictorial representation of the algorithm given in (3.4) is shown in Figure 3.1.

المنارة للاستشارات
www.manaraa.com

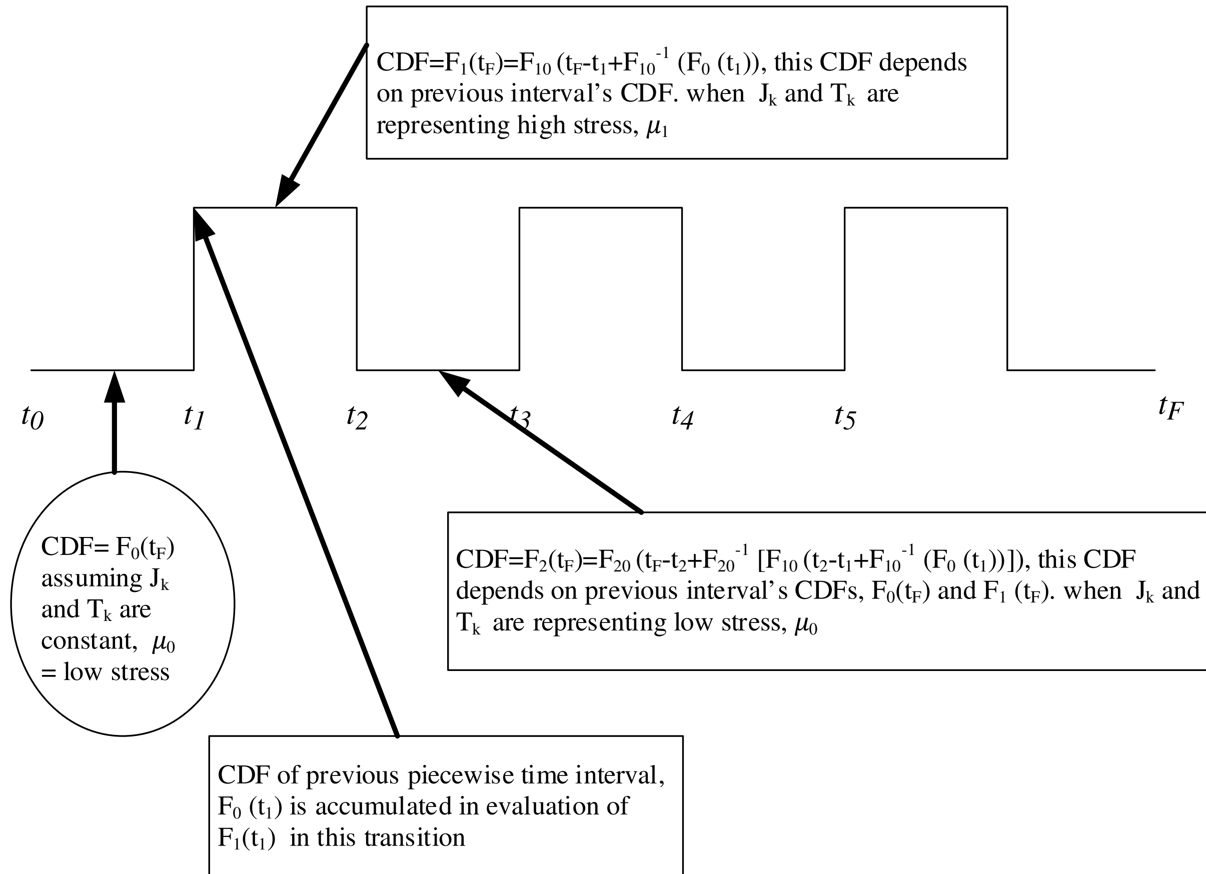

Figure 3.1: Modeling of time-dependent stress

It is assumed that for a time period the stress is changing as low stress and high stress. In any time instant, t_F, CDF, $F_0(t_F)$ is calculated according the value of current density J_K and temperature T_K at that specific time instant. In Figure 3.1, J_0 and T_0 correspond to low stress in first time interval, and J_1 and T_1 correspond to high stress in the next interval which are constant in that specific period. During the transition from low stress to high stress, the CDF of the

المنارة للاستشارات
www.manaraa.com

previous piecewise interval $F_0(t_1)$ is accumulated to evaluate new CDF, $F_1(t_1)$. During the high stress application, in any time instant this new CDF, $F_1(t_F)$ is defined as, $F_1(t_F)=F_{10}(t_F-t_1+F_{10}^{-1}(F_0(t_1))$. In this way, in each time interval CDF is evaluated accumulating the effect of previous time interval's CDF, which finally gives a continuous non decreasing CDF function. Using equation (3.4) to model the time-dependent stress, four different time-dependent stress simulations were made. These time dependent stress intervals are shown in the Figure 3.2 to Figure 3.5.

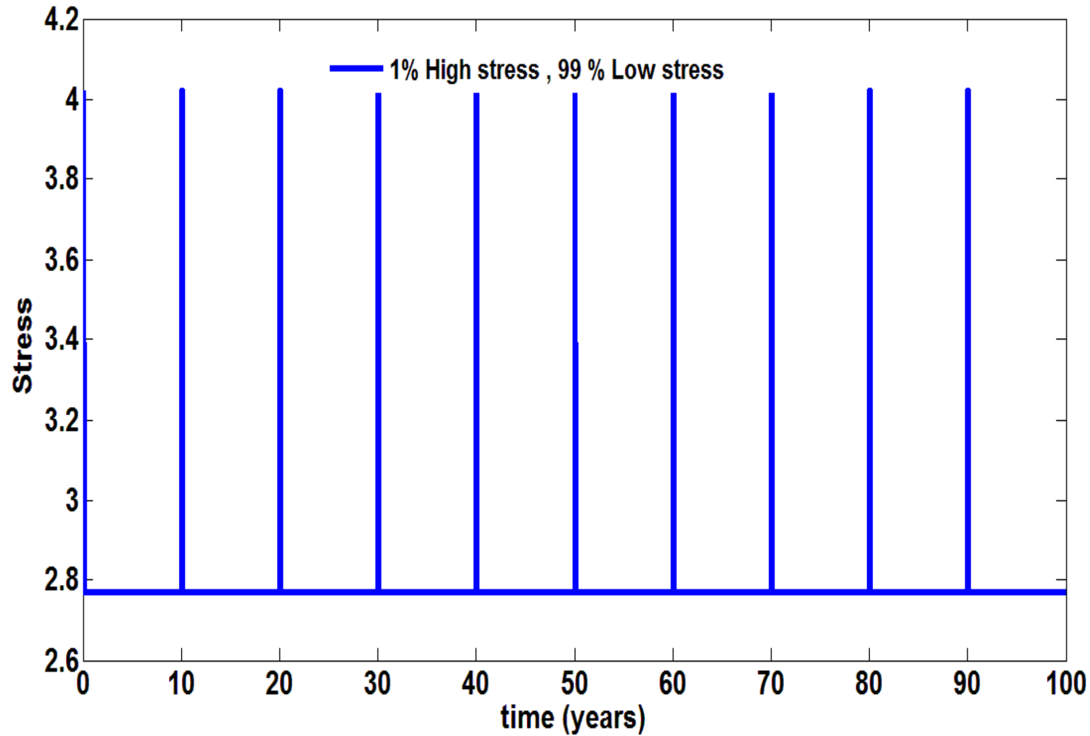

Figure 3.2: 1% high stress and 99% low stress duty cycle

المنارة للاستشارات
www.manaraa.com

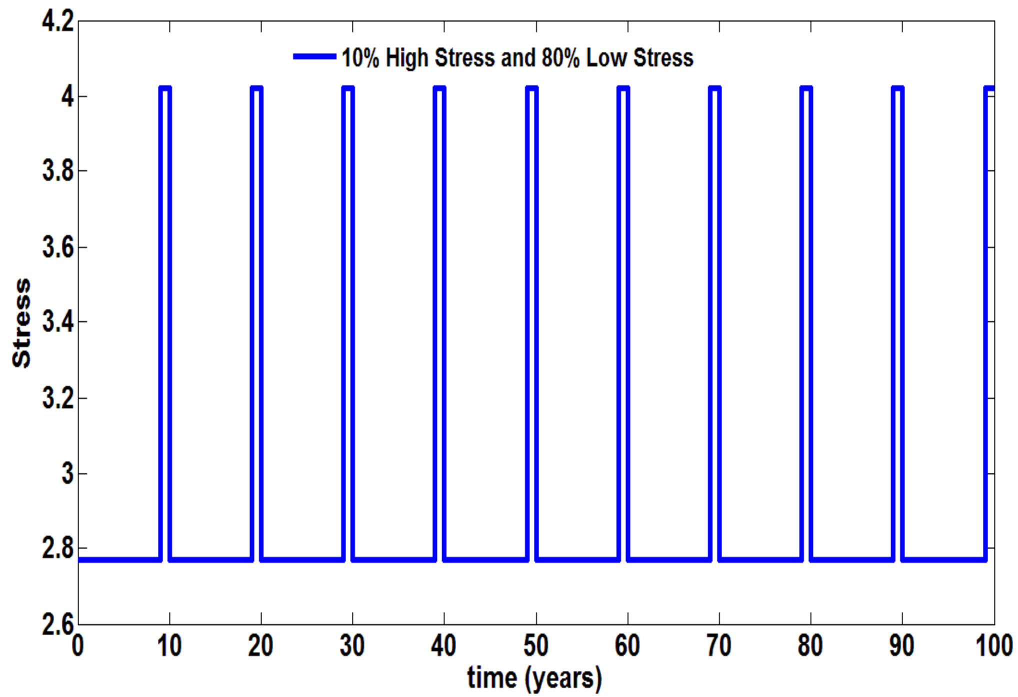

Figure 3.3: 10% high stress and 80 % low stress duty cycle

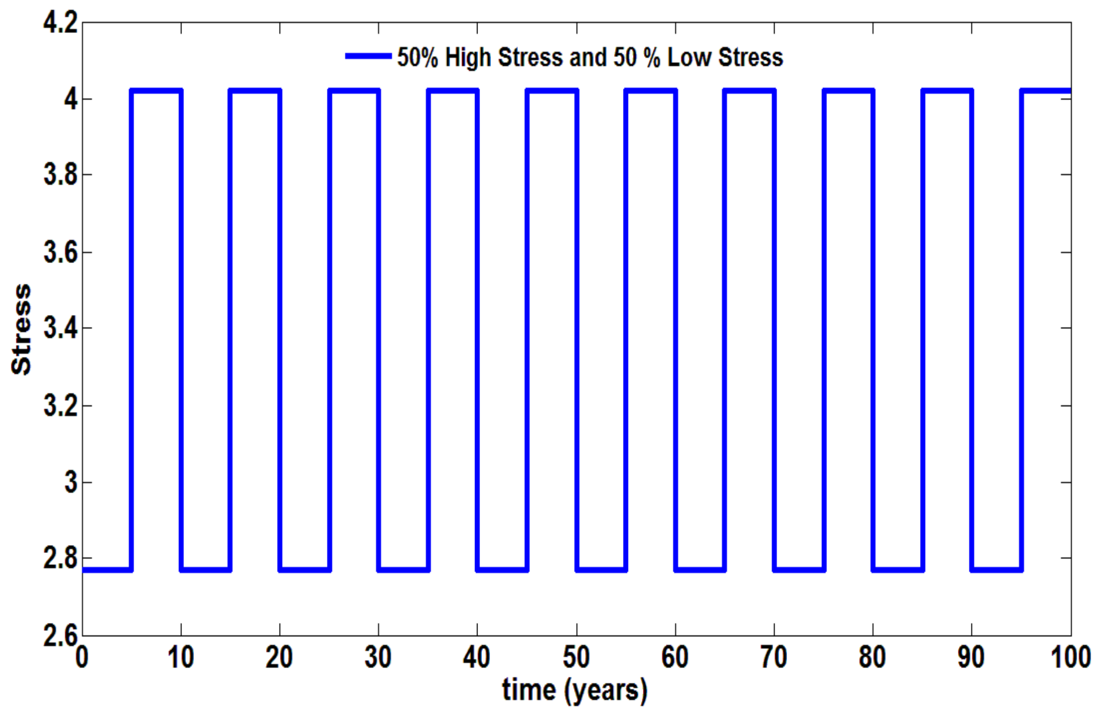

Figure 3.4: 50% high stress and 50 % low stress duty cycle

المنارة للاستشارات
www.manaraa.com

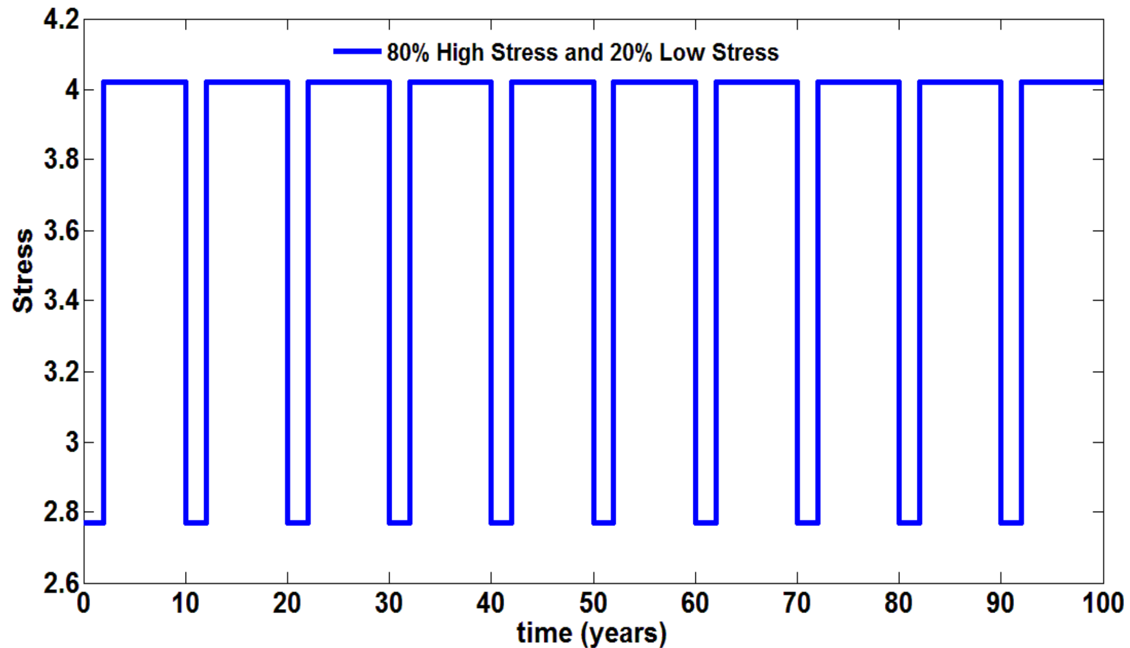

Figure 3.5: 80% high stress and 20 % low stress duty cycle

Simulation results are shown in Figure 3.6 to Figure 3.9. Results are summarized in Table 3.1. In all cases, there were 11 different stress intervals which correspond to 10 stress transition times and two different stress levels, one termed the high stress and the other termed low stress. All time-dependent stress tests started with the low stress condition and then toggled between the high stress and low stress levels at each stress transition time. The high stress condition corresponds to $J=J_{MAX}$ and $T=T_{MAX}$ as identified above. The low stress condition corresponded to $J=0.85J_{MAX}$ and $T=T_{MAX}-10^{o}C$. These low stress conditions are still likely much higher than what would be experienced in many applications. The lifetime of metal interconnect under time varying stress are observed in Figure 3.6 to Figure 3.9.

المنارة للاستشارات
www.manaraa.com

Table 3.1 Different MTF in Time Variant Stress

High Stress	**Low Stress**	
Current Density (J_{max}) 3 MA/ cm^2	Current Density (85% J_{max}) 2.55 MA/cm^2	
Temperature (T_{max}) 110 ^{0}C	Temperature(91% T_{max}) 110 ^{0}C-10^{0}C	
μ (High stress) (2.77)	μ(Low stress) (4.02)	MTF (years)
0% DC	100% DC	55.68
1% DC	99% DC	54.46
10% DC	90% DC	45.75
50% DC	50% DC	26.68
80% DC	20% DC	18.84
100% DC	0% DC	15.96

المنارة للاستشارات
www.manaraa.com

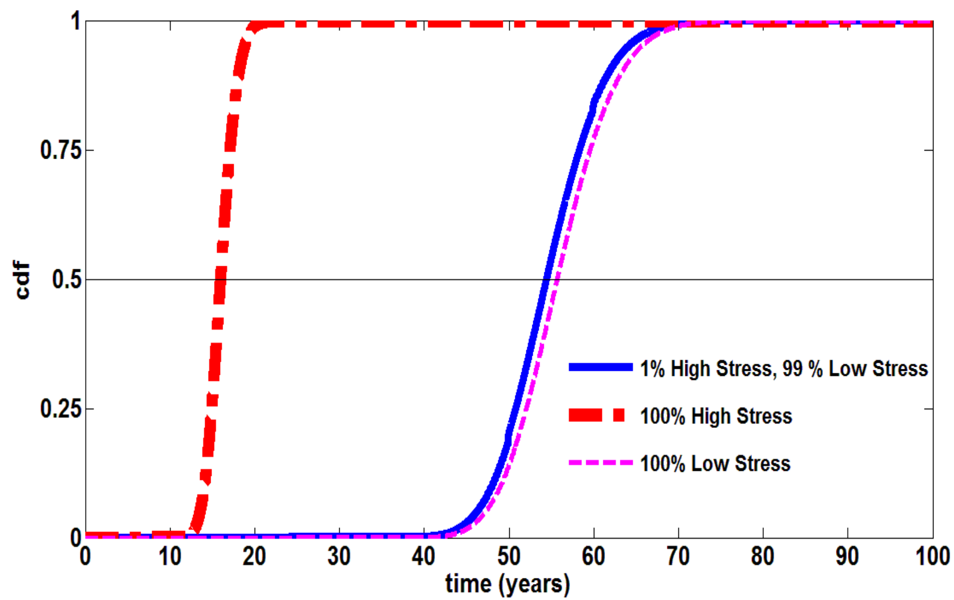

Figure 3.6: CDF vs time when high stress with 1% duty cycle (DC) and low stress with 99 % DC

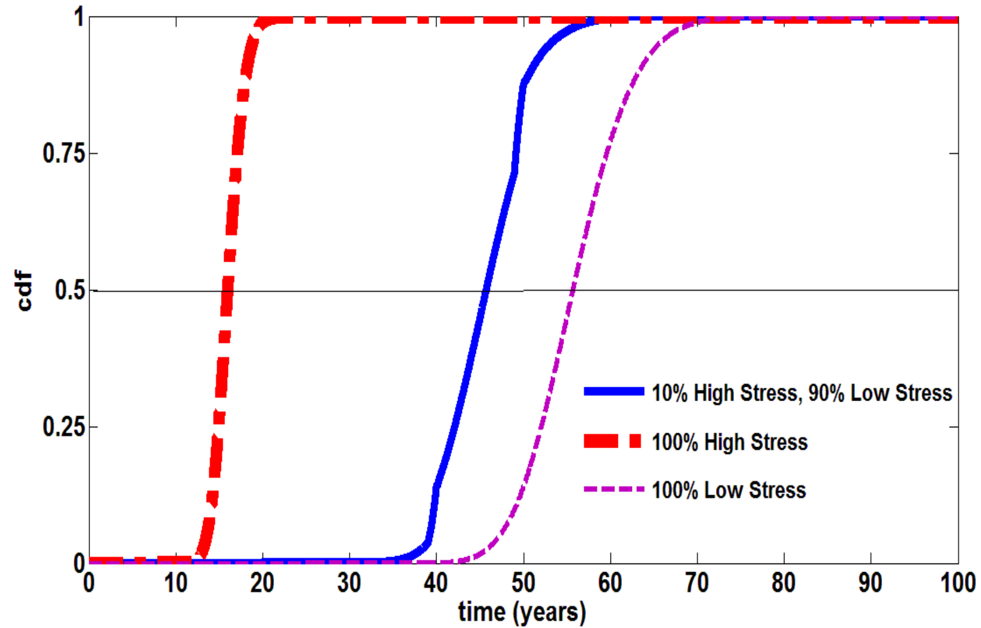

Figure 3.7: CDF vs time when high stress with 10% DC and low stress with 90 % DC

المنارة للاستشارات
www.manaraa.com

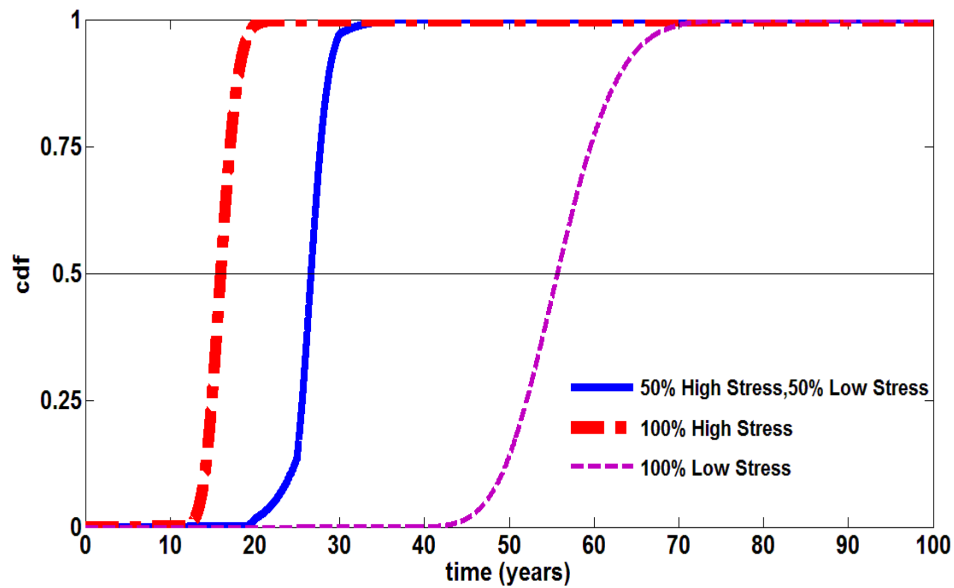

Figure 3.8: CDF vs time when high stress with 50% DC and low stress with 50 % DC

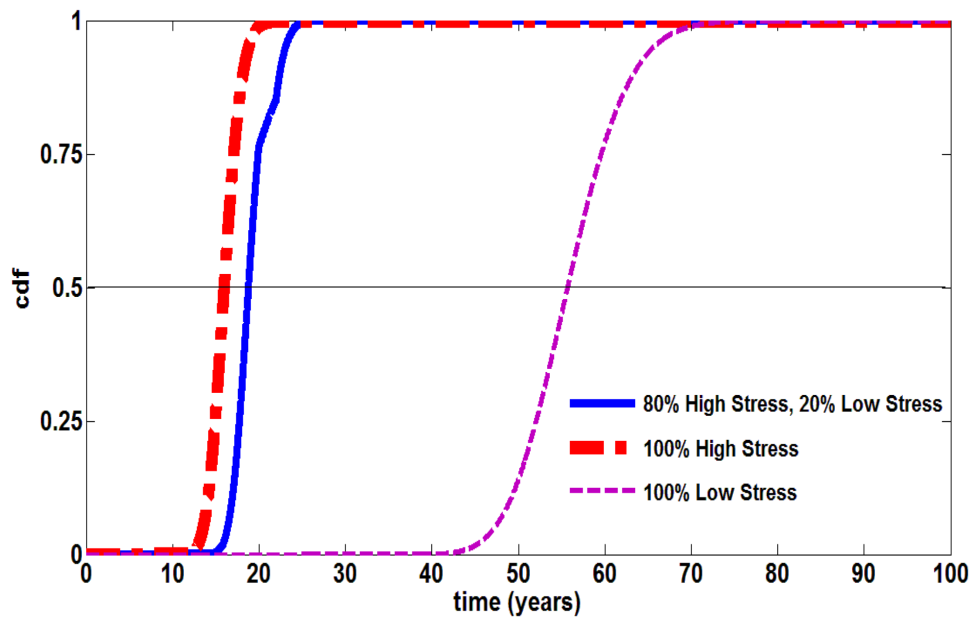

Figure 3.9: CDF vs time when high stress with 80% DC and low stress with 20 % DC

المنارة للاستشارات

www.manaraa.com

In the results shown in Figure 3.6, there was a 1% high stress and a 99% low stress with the first stress transition occurring at 9.9 years the second occurring at 10.0 years and with the high and low stress intervals remaining constant through the remaining stress transitions. The MTF under the constant high stress and constant low stress range between 15.96 years and 55.68 years with the 1% time varying high stress corresponding to a MTF of 54.46 years. In the results shown in Figure 3.7, there was a 10% high stress and a 90% low stress with the first stress transition occurring at 9 years and the second occurring at 10.0 years. This time varying stress has a MTF of 45.75 years. In the results shown in Figure 3.8, there was a 50% high stress and a 50% low stress with the first stress transition occurring at 5 years and the second occurring at 10.0 years. The MTF was 26.68 years. In the results shown in Figure 3.9, there was an 80% high stress and a 20% low stress with the first stress transition occurring at 2 years and the second occurring at 10 years. The MTF was 18.84 years.

It can be concluded from these simulations that including the time-varying stress when predicting the actual MTF can have a dramatic effect on the actual MTF with well over a 300% change in the MTF with even a relatively modest time-dependent change in stress.

Also from the above results it is shown in Figure 3.10 that to maintain the MTF to within ±10% of the target MTF, the temperature must be measured to within $\pm 1.6^0$C under the assumption that current density is fixed to 3 MA/ cm^2. The targeted MTF in this case is 16 years, to obtain ±10% of this MTF(14.4 years and , 17.6 years) with fixed current density, temperature increases from 110^0C to 111.6^0C and decreases to 108.6 ^{0}C respectively. Therefore, the accuracy of the temperature sensor has to be very high.

المنارة للاستشارات

www.manaraa.com

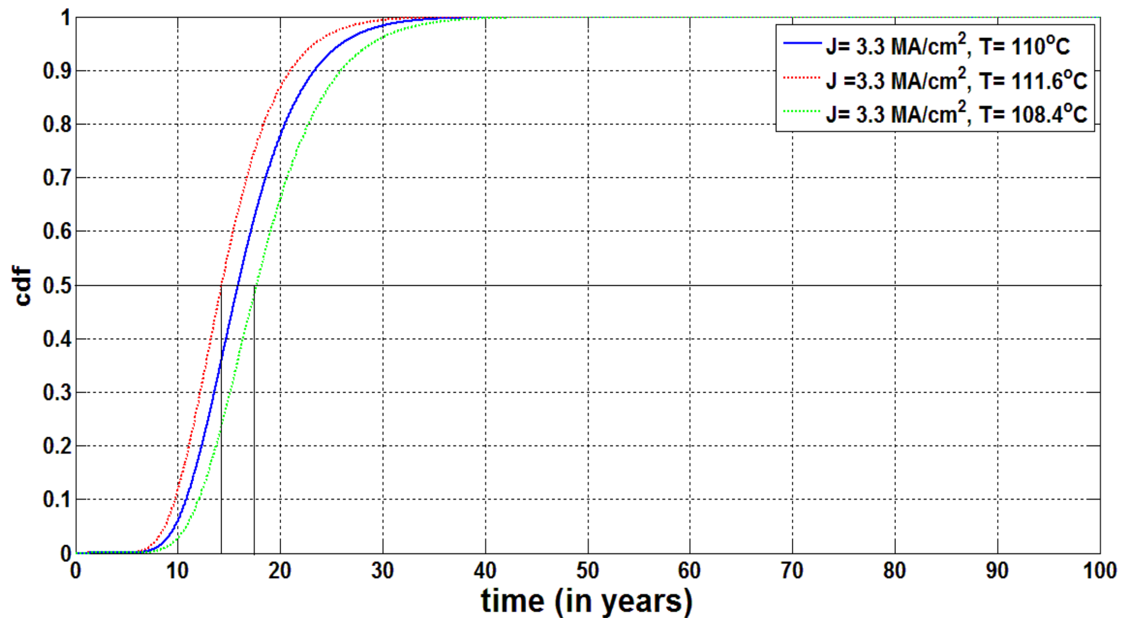

Figure 3.10: CDF vs time when MTF is ±10% of the target MTF, temperature is within $\pm 1.6^{0}$C

3.1 Conditional Reliability and Conditional MTF

The derivations in this work were made under the assumption that the time-varying stress conditions were known prior to putting a system into use. In actuality, the time-varying stress will depend upon how each specific system is used. Thus, there is some probability that the system will fail under the time varying stress conditions and this probability increases with the time that the system is used. It would be more useful to determine the conditional CDF or the conditional MTF under actual varying stress conditions if a real-time power/thermal management algorithm is adopted. In high-reliability systems, the probability of failure throughout the specified life of the system will be small and in these cases the previous analysis of the MTF will provide a close approximation to the MTF throughout the useful life of the system. The conditional reliability is calculated using equation (3.4) and shown in Figure 3.11.

المنارة للاستشارات

www.manaraa.com

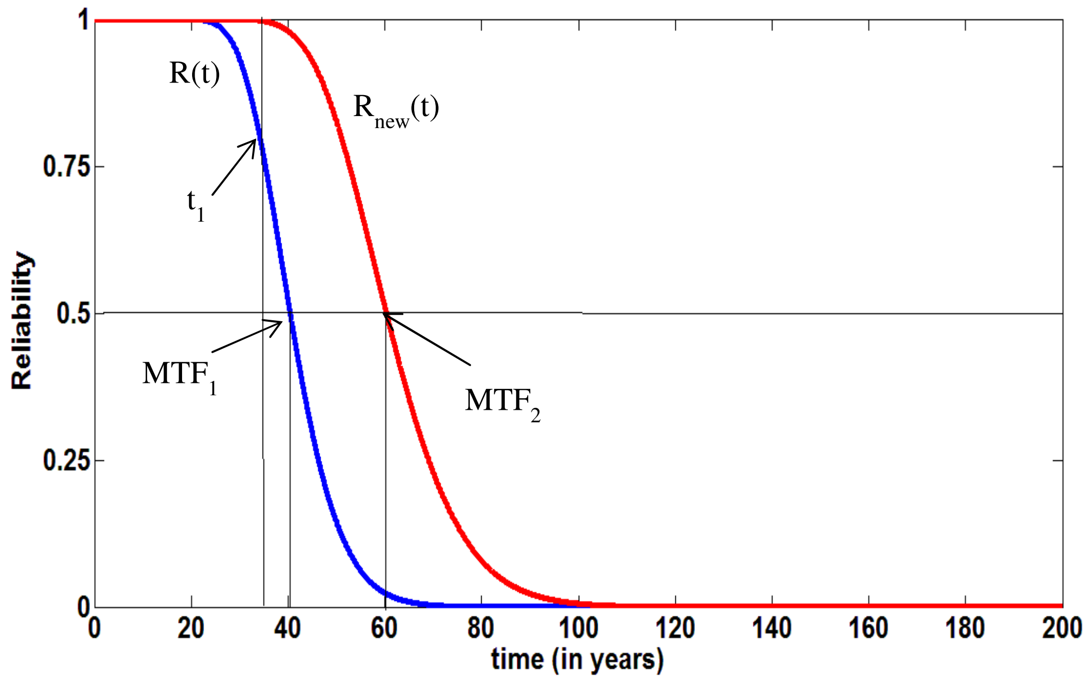

Figure 3.11: Conditional reliability function to measure conditional MTF

If the metal interconnect is survived to time t_1 and if $R_{new}(t)$ is the conditional reliability at time t, where $t_1 < t$, the conditional reliability can be calculated as [22],

$$R_{new}(t) = \frac{R(t-t_1)}{R(t_1)} \tag{3.5}$$

Once we evaluate $R_{new}(t)$, the previous reliability function, $R(t_1)$ can be discarded. The new conditional MTF of the metal interconnect can be obtained in from new conditional reliability function in following way, $R_{new}(t_F) = 0.5$ and $t_F = R_{new}^{-1}(0.5)$ (3.6)

where t_F is failure time.

المنارة للاستشارات
www.manaraa.com

3.2 Equivalent Age Stress

Often systems are designed under the assumption that the stress will be constant throughout the life of the system. This term is called as nominal use stress. If the actual stress is more than the nominal use stress, the system will age more rapidly than under nominal use stress and if the actual stress is less than the nominal use stress, the system will age less rapidly than under normal use stress. When predicting the reliability of a system under time-varying stress, the sequence $\langle F_{k-1}(t_k) \rangle_{k=1}^{\infty}$ was used as an indicator of the wear and the only memory in the system required to predict stress in the interval $t_k<t_F<t_{k+1}$ was $F_{k-1}(t_k)$. But $F_{k-1}(t_k)$ may give little insight into whether the accumulative stress in this interval is larger or smaller than that under normal use. The equivalent age stress will provide more insight into how the stress is affecting the aging of the system. If the nominal use stress is not time dependent and characterized by the CDF $F_{NOM}(t_k)$ and the nominal MTF is given by

$$MTF_{NOM}=A_0\left(J_{NOM}-J_{CRIT}\right)^{-N} e^{\left(E_a/kT_{NOM}\right)} \tag{3.7}$$

then we can define the equivalent aging time at each time $t_{AGE,k}$ by

$$\langle t_{AGE,k} \rangle_{k=1}^{\infty} = \langle F_{NOM}^{-1}\left(F_{k-1}(t_k)\right) \rangle_{k=1}^{\infty} \tag{3.8}$$

And the normalized equivalent aging stress change, $t_{EAS\text{-}NORM,k}$ by

$$\langle t_{EAS\text{-}NORM,k} \rangle_{k=1}^{\infty} = \left\langle \frac{t_k - t_{AGE,k}}{MTF_{NOM}} \right\rangle_{k=1}^{\infty} \tag{3.9}$$

There is a 1-1 relationship between the equivalent aging time and the wear indicator $F_{k-1}(t_k)$ or correspondingly between the normalized equivalent aging stress change and $F_{k-1}(t_k)$. Thus, instead of storing the single wear indicator variable $F_{k-1}(t_k)$ to calculate the MTF, one can

www.manaraa.com

alternatively store either the equivalent aging time or the normalized equivalent aging stress change. The latter would be more useful in assessing the accumulative effects of the actual stress on the system. Whereas the sequence $\langle t_{AGE,k} \rangle_{k=1}^{\infty}$ is monotone, the sequence $\langle t_{EAS\text{-}NORM,k} \rangle_{k=1}^{\infty}$ can take on either positive or negative values. When $t_{EAS\text{-}NORM,k}$ is positive, the system is wearing faster than the nominal use system and when it is negative, the system is wearing slower than the nominal use system. The magnitude of this quantity is an indicator of how much faster or slower the system is wearing.

3.3 Relation Between MTF and FIT

Although the MTF is a statistic that characterizes the failure time or reliability of a device, the MTF is generally much longer than the useful operating life of an integrated circuit. Industry is often more concerned about the number of early failures of a component since the cost of returns during a short warranty period is based upon the early failures. For a given distribution, there is a known relationship between the number of early failures in any interval and the MTF. Thus, in reliability electronics applications, instead of the MTF, industry prefers to use the statistic FIT (failures in time) as a measure of the failure rate. The FIT is defined as the hazard function in units of (1/ hours) x 10^9 [18] and is given by the expression,

$$FIT = \frac{f(t_F)}{1 - F(t_F)} \times 10^9 \tag{3.10}$$

where $f(t_F)$ is probability density function and $F(t_F)$ is cumulative density function of the time to failure considered in the previous sections of this thesis. They are related by the well-known equation

المنارة للاستشارات
www.manaraa.com

$$F(t_F) = \int_0^{t_F} f(t_F)dt \tag{3.11}$$

As discussed previously, the MTF (Median time to failure) can be expressed as

$$\text{MTF} = F^{-1}(0.5) \tag{3.12}$$

Assuming a lognormal distribution of the time to failure, $f(t_F)$ is given by the expression

$$f(t_F) = \frac{1}{2\pi\sigma t_F}\exp\left(-0.5\left(\frac{\ln t_F - \mu}{\sigma}\right)^2\right) \tag{3.13}$$

Then $F(t_F)$ is calculated using equation (3.11). Replacing $f(t_F)$ and $F(t_F)$ values in equation (3.10) the FIT values can be calculated. Using equation (3.10) and equation (3.12), the relation between MTF and FIT can be obtained. This relationship is shown graphically for μ is varying from 1.61 years to 2.07 years and σ=0.35 in Figure 3.12 for three different time intervals.

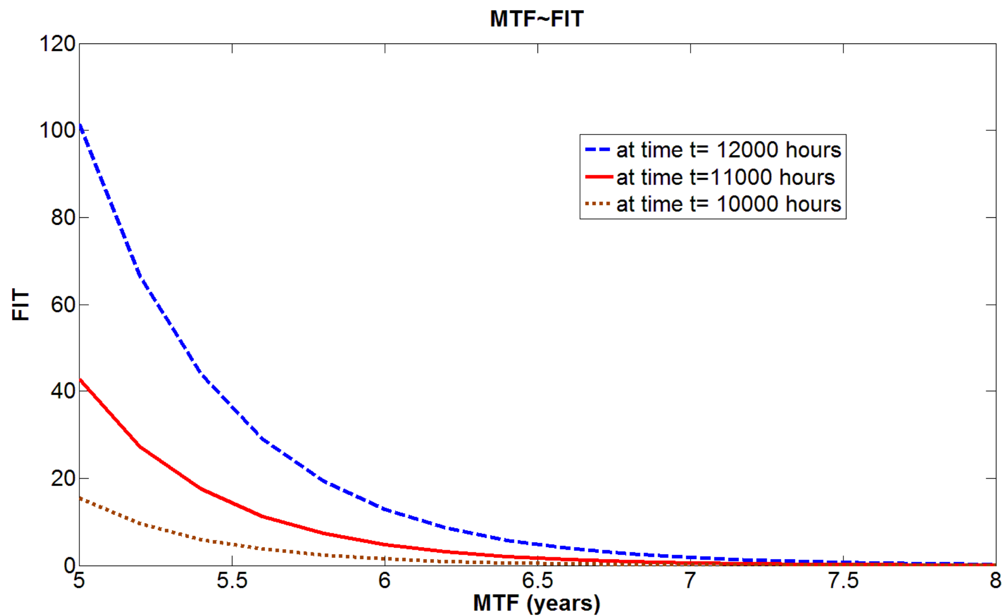

Figure 3.12: Relation between MTF and FIT in different values of experiment time

المنارة للاستشارات
www.manaraa.com

Some well-known properties of the relationships between the MTF and the FIT can be observed from Figure 3.12. The FIT values are decreasing with respect to ascending values of MTF and FIT values increase with increments of the experiment time for a specific MTF value. At this stress level and with the specified shape factor, when the MTF is 5 years, the FIT at 10000 hours is 14.5, at 11000 hours it is 42.7, and at 12000 hours the FIT is 101.1. The same plot is shown with a FIT log scale in Figure 3.13.

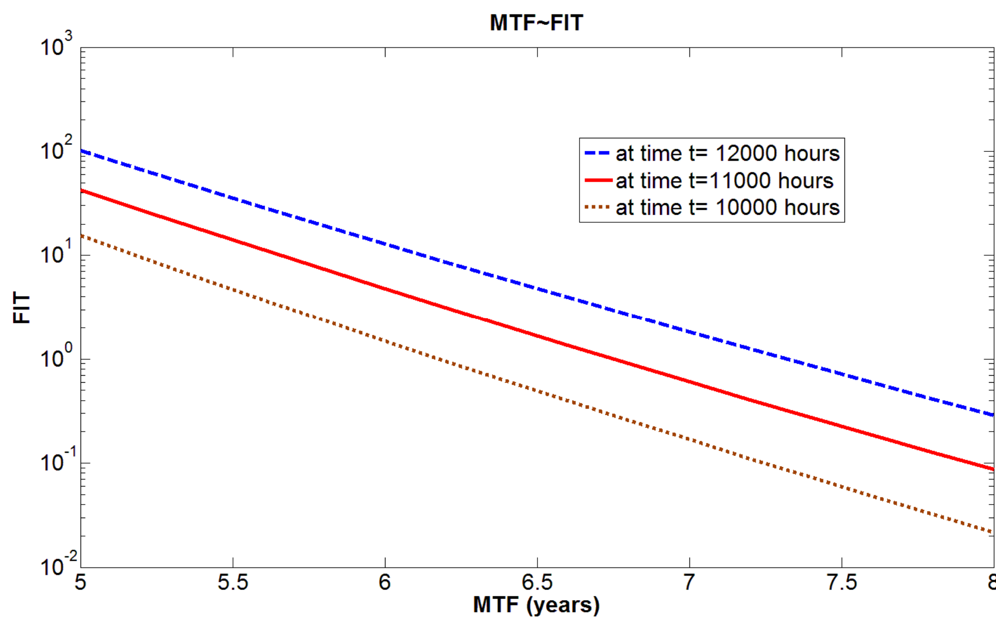

Figure 3.13 : Relation between MTF and log (FIT) in different experiment time

3.4 Practical Considerations and Open Issues

From a practical viewpoint, good modeling of the lifetime of an interconnect in the presence of a large number of different stress intervals will require a large number of intervals. More realistically the accumulated "wear" at the end of the first stress interval will be very small

المنارة للاستشارات
www.manaraa.com

and, even if a very large number of stress intervals are present, the accumulated “wear” after a large number of stress intervals will also be small if the interconnect is to have good reliability.

The issue of what distribution best models the wear in an interconnect deserves some additional attention. In the presentation of the previous sections, a lognormal distribution with a shape parameter of $\sigma=0.3$ was used as an example. Most discussions in the literature that do present measured electromigration results focus only on the MTF and do not address what distribution was used nor how well the MTF model fits the data. As is the case for accurate reliability predictions in the presence of constant stress, accurate reliability prediction in the presence of time-dependent electrical and thermal stress requires not only good parameters in the MTF equations but good models for the distribution function as well.

المنارة للاستشارات
www.manaraa.com

CHAPTER 4 - RELIEABILITY MODELING OF METAL INTERCONNECT WITH ELECTRICAL, THERMAL AND THERMAL GRADIENT STRESS

In this chapter, an empirical statistical model will be introduced that attempts to combine the effects of electrical stress, thermal stress, and thermal gradient stress (ETTG) on the reliability of interconnects. The purpose of this model is to obtain an estimate of the level of degradation in reliability that will occur in the presence of significant levels of combined ETTG stress and to obtain an estimate of the accuracy needed for on-chip temperature and temperature gradient sensors if they are used as part of a power/thermal management algorithm to manage the reliability of an integrated circuit.

Though static thermal gradient stress is known to limit lifetime of an interconnect, there is little in the literature to suggest how this should be incorporated into a reliability model that jointly includes the effects of current stress, thermal stress, and thermal gradient stress. Lacking such a model, we have empirically included the thermal gradient as a stress parameter along with temperature and current density by modifying the MTF equation of Black equation (2.6) as a separable function of J, T, and the thermal gradient ΔT as,

$$MTF = \begin{cases} \infty & J < J_{CRIT} \\ A_0 \left(J - J_{CRIT}\right)^{-N} e^{(E_a/kT)} \left(1 + a_1 \Delta T + a_2 \Delta T^2\right) & J > J_{CRIT} \end{cases} \quad (4.1)$$

The parameters in the polynomial equation are obtained by fitting experimental MTF measurements [10] to actual temperature gradients. It will be assumed that the CDF can be expressed using the lognormal distribution as [18]

$$F_{LNi}\left(t_F, \mu_i, \sigma\right) = F_{N01}\left(\frac{\ln\left(t_F\right) - \mu_i}{\sigma}\right) \quad (4.2)$$

www.manaraa.com

where $$\mu_i = \ln\left(\left(A_0 \left(J_i - J_{CRIT}\right)^{-N} e^{(E_a/kT_i)}\right)\left(1 + a_1 \Delta T + a_2 \Delta T^2\right)\right) \quad (4.3)$$

and where F_{N01} denotes the CDF of the Normal (0,1) random variable. The parameter σ determines the steepness of the CDF in the region around $t_F = F^{-1}(0.5)$ and ln(x) is the natural logarithm function.

Existing power/thermal management algorithms typically throttle the speed of operation when the temperature reaches a predetermined trigger level and this level is often based upon the assumption that the current density stress is maintained at some maximum nominal level, J_{NOM}. By throttling the speed, the temperature can ideally be maintained at or below the trigger temperature, denoted as T_{NOM}. The trigger temperature is typically established so that if the device is operated continuously at T_{NOM} and the current is maintained continuously at J_{NOM} the circuit will meet a target MTF. Some power/thermal management algorithms have a single temperature sensor and some use multiple on-chip temperature sensors. In the latter case, the power/thermal management algorithm will ideally keep the temperature at each sensor location at or below T_{NOM}.

With existing approaches to power/thermal management, thermal gradient information is not a part of reported speed throttling processes and if large temperature gradients are present, the temperature-based throttling will not be adequate for meeting target MTF goals. If on-chip temperature gradient sensors are strategically placed on a die at locations where thermal gradients are likely to be most critical, the power/thermal management algorithm can be modified to also throttle speed whenever the thermal gradients meet a trigger gradient value. This trigger gradient is denoted as ΔT_{NOM}. The analogous power/thermal management strategy would be to pick both T_{NOM} and ΔT_{NOM} so that if the device is operated continuously at the

المنارة للاستشارات
www.manaraa.com

ETTG stress level of J_{NOM}, T_{NOM}, and ΔT_{NOM}, then the circuit will meet a target MTF goal. To implement such an algorithm, a model of the MTF that incorporates the ETTG stress conditions is needed as well as both temperature and temperature gradient sensors.

Lacking an established model, we will use the empirical model of (4.1) which incorporates the ETTG stress parameters. Since the MTF is quite sensitive to small changes in stress conditions, it is also necessary to determine the accuracy requirements for both the temperature sensors and the temperature gradient sensors. Now an estimate of the thermal gradient stress parameters, a_1 and a_2 in (4.1) is obtained. In [10], Nguyen et. el. studied the effects of thermal gradients on an AlSi(1%)Cu(.04%) interconnect with an accelerated lifetime test. In their study, the temperature at the hot side of the interconnect was maintained at 202^0C by a local heater and the temperature at the low side was adjusted in four separate tests using oven to create thermal gradients of 0, 0.09, 0.19, and 0.28^0C/µm shown in Figure 4.1. In these tests, the MTF decreased from 46.6h when there was no gradient to 41.8h, 19.8h, and 4.1h respectively with the larger thermal gradients mentioned in Table 4.1.

المنارة للاستشارات
www.manaraa.com

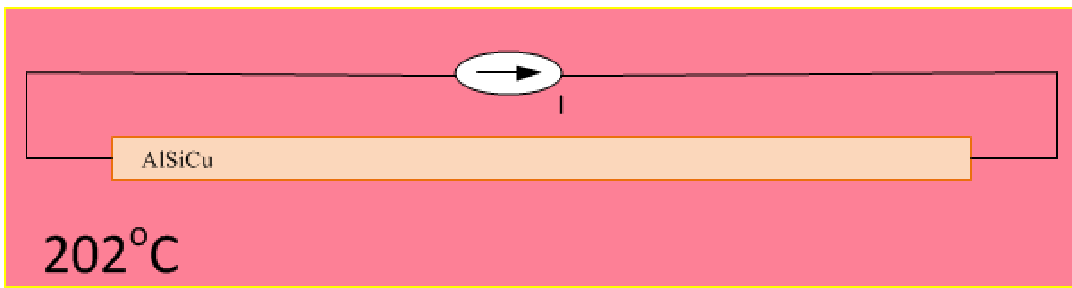

Constant Static Electro-Thermal Stress

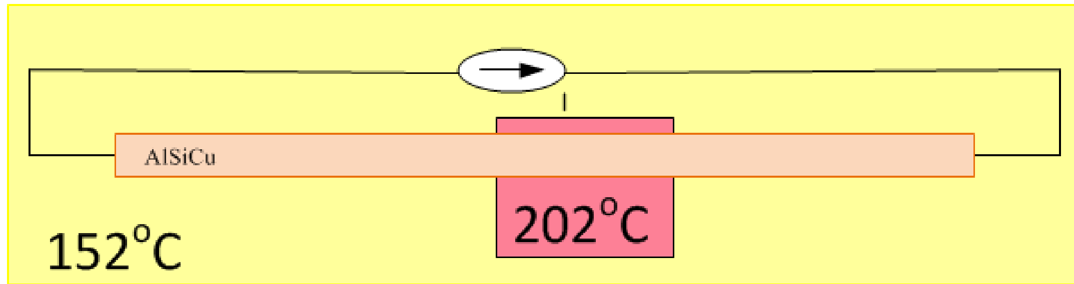

Static Electro-Thermal Stress Gradient 0.19°C/µm

Figure 4.1 Arrangement to produce thermal gradient

Table 4.1 : Different Temperature Gradient Conditions and Corresponding Time to Failure (TTF) [10]

Condition	Heater Temp (Hot side) (^{0}C)	Thermal Gradient, ΔT , (^{0}C/µm)	Oven Temp (Low side) (^{0}C)	TTF (hrs)
Uniform	-	0	202	46.6
Tgrad1	202	0.09	177	41.8
Tgrad2	202	0.19	152	19.8
Tgrad3	202	0.28	127	4.3

المنارة للاستشارات
www.manaraa.com

With these measurements and the assumption that the MTF is a separable function of J, T, and the gradient ΔT, the second-order polynomial fit parameters a_1 and a_2 of (4.1) can be estimated. An estimate of these parameters is a_1=-2.629 and a_2=-2.088.

These fit parameters are used to predict the MTF under different ETTG conditions in a state of the art process. Since it is recognized that the metal characteristics may be somewhat different and the assumption of a separable function for the MTF is strictly empirical, there will be some model errors but lacking experimental data for predicting the effects of thermal gradients, the results obtained should at least be indicative of what could happen in these processes when thermal gradients are present. Typical values for stress variables J_{NOM} and T_{NOM} for the 0.45 nm technology node are 3 MA/cm^2 [19] and 110 ^{0}C [20] respectively. Using these stress variables, and assuming a lognormal distribution with shape factor of σ=0.3, with typical values for A_0 and E_a in (4.3), we obtain the CDF plots shown in Figure 4.2 under the four gradient conditions 0, 0.09, 0.19, and 0.28^{0}C/μm. The corresponding MTF for the four gradient conditions are summarized in Table 4.2.

المنارة للاستشارات

www.manaraa.com

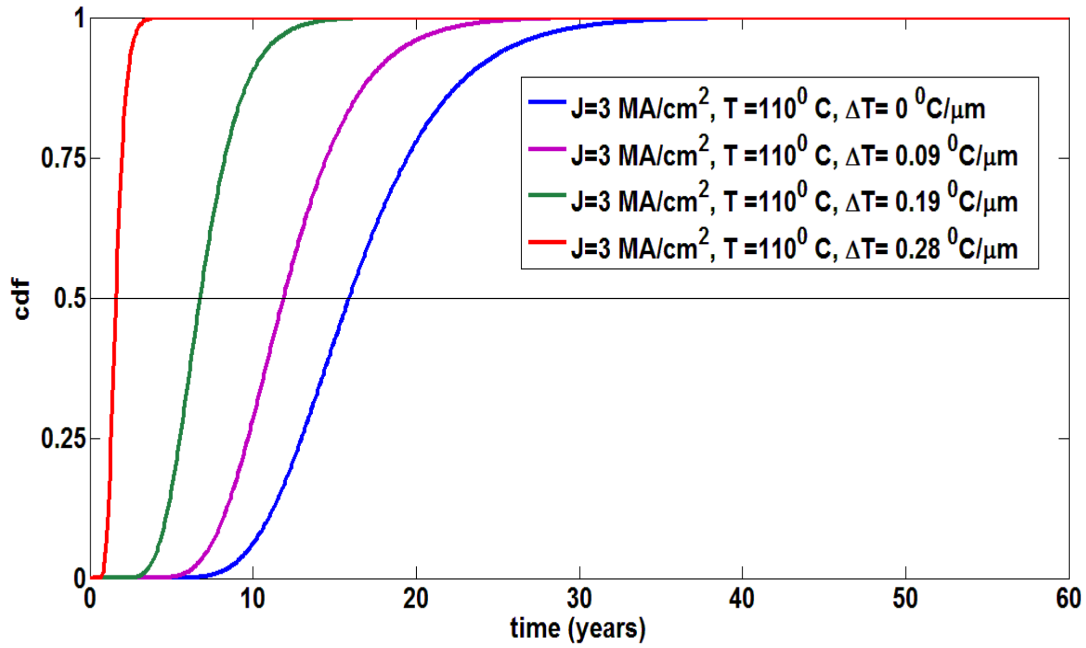

Figure 4.2: CDF plots under different ΔT in T_{NOM} and J_{NOM} conditions

From these results it is observed that under a constant ambient temperature and current density condition, when the thermal gradient is increased from 0^0C/µm to 0.28^0C/µm, the MTF has decreased by factor of approximately 10. As expected, this is the same relative decrease that was reported in [10].

Table 4.2. MTF in Different ΔT with Normal Stress

Current Density (J) 3 MA/cm^2	(under Temp Gradient (ΔT) ^{0}C/µm	µ	MTF (years)
Temperature (T) 110 ^{0}C	0	2.76	15.8
	0.09	2.47	11.8
	0.19	1.91	6.8
	0.28	0.46	1.6

المنارة للاستشارات
www.manaraa.com

A comparison will now be made with the degradation in reliability due to thermal gradients with changes in reliability due to changes in electrical or temperature stress. In previous chapter the effects of changes in electrical and thermal stress were considered using the distribution function that differed from that used here with the exception that temperature gradient effects were ignored (i.e. with $a_1=a_2=0$). These results are repeated in Figure 4.3 and the results are compared numerically in Table 4.3. Comparing the results in Table 4.2 and Table 4.3, it can be seen that a gradient of 0.09 ^{0}C/µm will cause about the same decrease in reliability as an increase of temperature of 6^{0}C in the absence of thermal gradients.

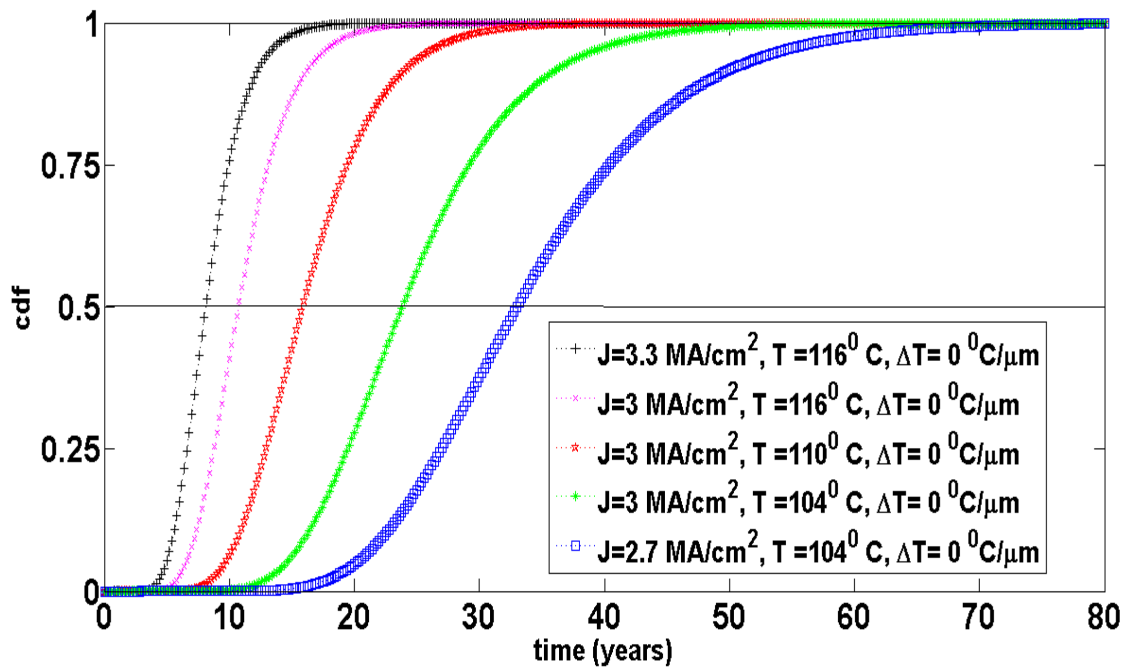

Figure 4.3: CDF plots under different T and J in absence of ΔT

المنارة للاستشارات
www.manaraa.com

Table 4.3. MTF in Different Stress in Absence of ΔT

Current Density (J) (MA/cm^2)	Temperature (T) ^{0}C	μ	MTF (years)
3.3(J+10%J)	110^{0}C+6^{0}C	2.09	8.2
3	110^{0}C+6^{0}C	2.37	10.8
3	110^{0}C	2.76	16
3	110^{0}C-6^{0}C	3.17	23.8
2.7 (J-10%J)	110^{0}C-6^{0}C	3.50	33

Figure 4.4, Figure 4.5 and Figure 4.6 compare the reliability under various combinations of the ETTG stress parameters. The results from these plots are summarized in Table 4.4, Table 4.5, and Table 4.6.

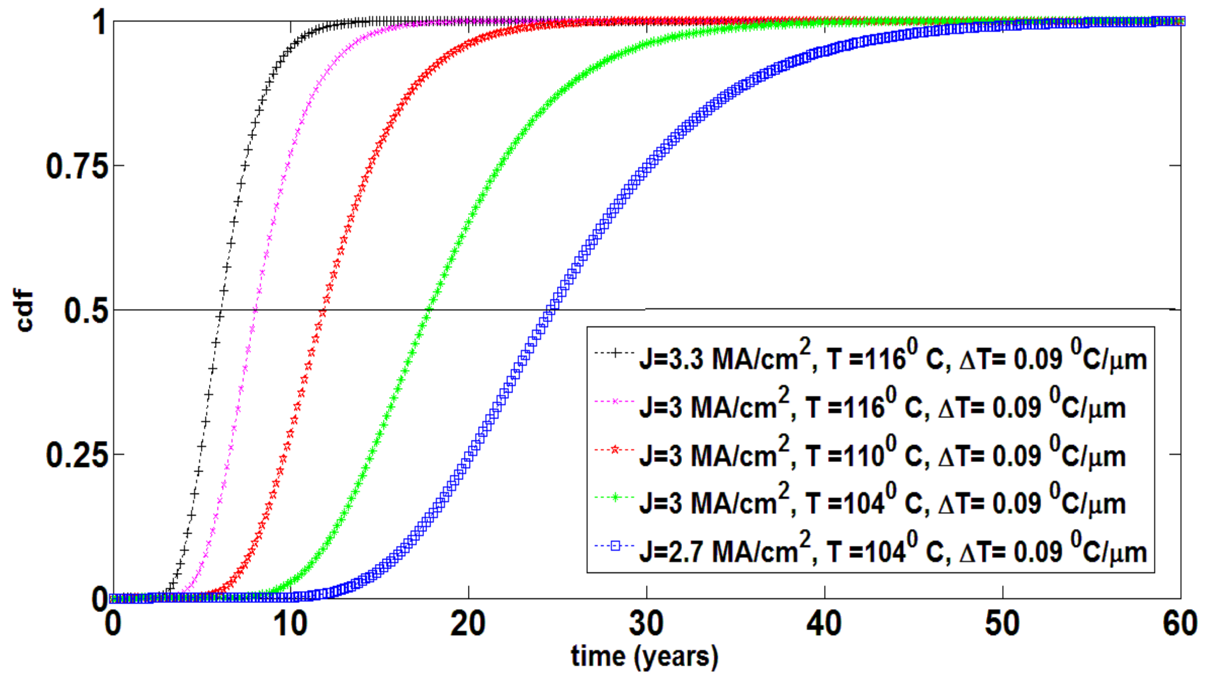

Figure 4.4: CDF plots under different T, J when ΔT = 0.09^0 C/μm

المنارة للاستشارات
www.manaraa.com

Table 4.4. MTF in Different Stress when $\Delta T = 0.09^0$ C/μm

Current Density (J) (MA/cm^2)	Temperature (T)	μ	MTF (years)
3.3(J+10%J)	110^0C+6^0C	1.80	6
3	110^0C+6^0C	2.08	18
3	110^0C	2.47	11.8
3	110^0C-6^0C	2.87	17.8
2.7 (J-10%J)	110^0C-6^0C	3.20	24.6

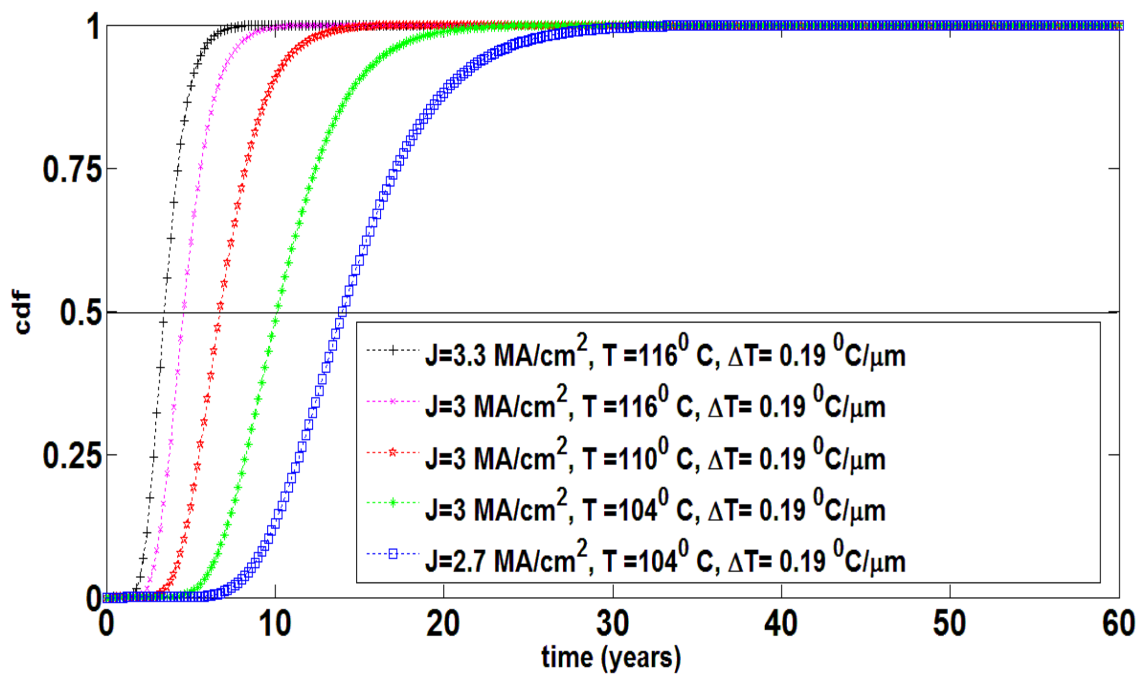

Figure 4.5: CDF plots under different T,J when $\Delta T = 0.19^0$ C/μm

المنارة للاستشارات
www.manaraa.com

Table 4.5. MTF in Different Stress when $\Delta T=0.19^0$ C/µm

Current Density (J) (MA/cm^2)	Temperature (T) ^{0}C	µ	MTF (years)
3.3(J+10%J)	110^0C+6^0C	1.24	3.4
3	110^0C+6^0C	1.52	4.6
3	110^0C	1.91	6.8
3	110^0C-6^0C	2.32	10
2.7 (J-10%J)	110^0C-6^0C	2.64	14

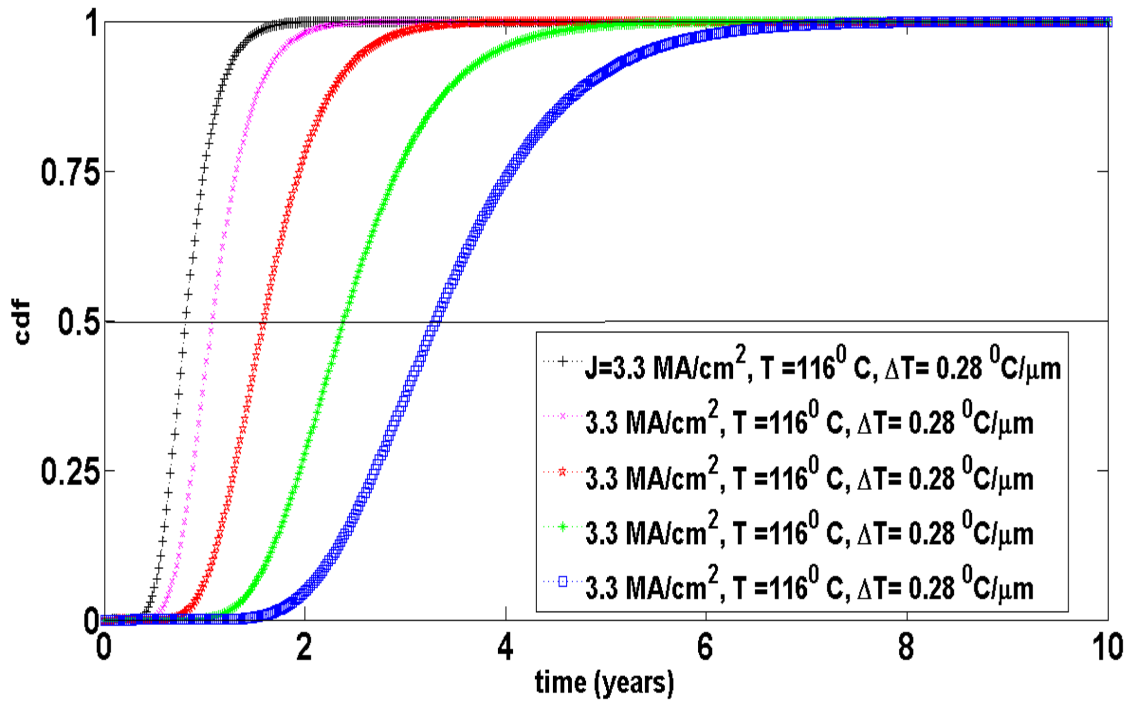

Figure 4.6: CDF plots under different T,J when $\Delta T = 0.28^0$ C/µm

المنارة للاستشارات
www.manaraa.com

Table 4.6. MTF in Different Stress when $\Delta T=0.28^0$ C/µm

Current Density (J) (MA/cm^2)	Temperature (T)	µ	MTF (years)
3.3(J+10%J)	110^0C+6^0C	-0.21	0.82
3	110^0C+6^0C	0.07	1.08
3	110^0C	0.46	1.6
3	110^0C-6^0C	0.87	2.38
2.7 (J-10%J)	110^0C-6^0C	1.19	3.32

From these simulation results, it can be observed that the MTF decreased from 33 years in the minimum stress condition of J=2.7MA/cm^2, T=104^{0}C, $\Delta T=0^0$C/µm to 0.82 years in the maximum stress condition J=3.3MA/cm^2, T=116^{0}C, $\Delta T=0.28^0$C/µm. This change in stress conditions is rather modest yet the change in reliability as characterized by the MTF is a factor of approximately 40. More importantly, it can be seen that each of the ETTG stress factors contribute significantly to the degradation in reliability.

The question naturally arises; How large of thermal gradient stresses are likely to occur? Though not quantized, thermal gradient stress in the 0.05^{0}C/µm has been reported in several papers focusing on hot spots. Other work, including that in [10] considers larger gradients. Lloyd [21] recently suggested thermal gradients well in excess of 1^{0}C/µm "will be found". Much of the reported thermal gradient information has focused on single-core processors. With multi-core processors now common, with increases in the number of cores, and with projections for increasing the total power dissipation on processors by a factor of 4 in the next few years while maintaining approximately the same die area, much larger thermal gradients can be expected and these thermal gradients will likely play increasingly important roles in the reliability of interconnects.

المنارة للاستشارات
www.manaraa.com

4.1 Accuracy Requirements for Temperature and Temperature Gradient Sensors

If power/thermal management algorithms use measured temperature and in the future, measured temperature gradient information to throttle operating frequency for the purpose of meeting reliability targets, the question naturally arises about how accurately these measurements need to be made.

It was shown in previous chapter that to maintain the MTF to within ±10% of the target MTF, the temperature must be measured to within $\pm 1.6^{0}$C. This requirement was established under the assumption that thermal gradients are not contributing to degraded lifetime. Using the lognormal model discussed above, it can be shown that if there are no errors in temperature measurement, and if a trigger thermal gradient of 0.2^{0} C/µm is established, then the accuracy of the thermal gradient sensor must be 0.011^{0}C/µm to maintain ±10% accuracy in the MTF as shown in Figure 4.7.

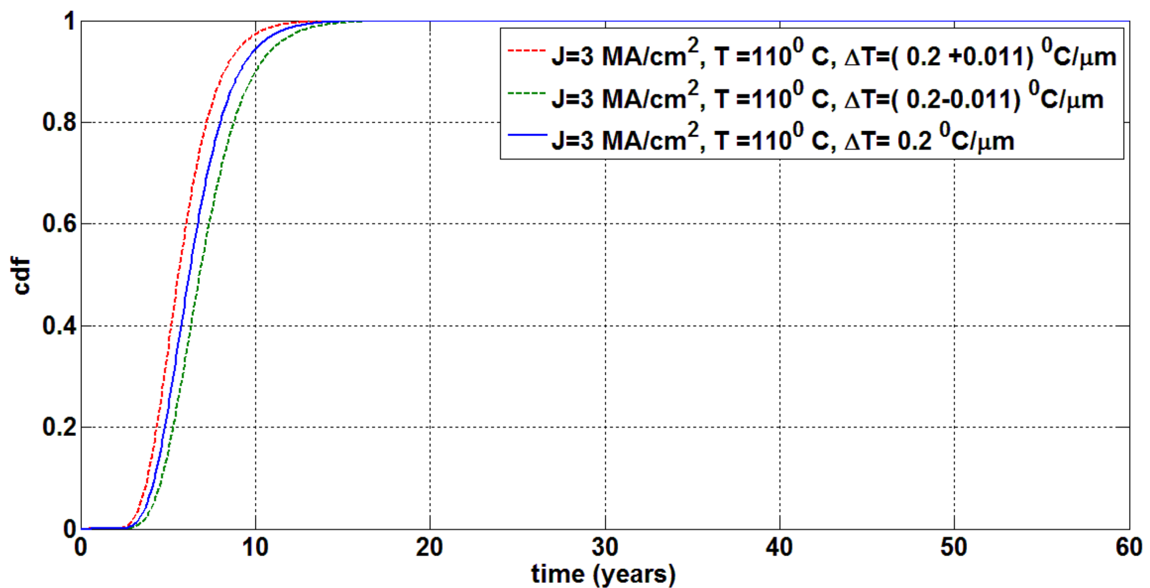

Figure 4.7: CDF vs time when MTF is ±10% of the target MTF under fixed current density and temperature measurement and temperature gradient is within $\pm 0.011^{0}$C/µm

المنارة للاستشارات
www.manaraa.com

As shown in Figure 4.7, the targeted MTF in this case is 6.1 years when current density, J=3 MA/cm^2, temperature, T=300^{0}C and temperature gradient ΔT = 0.2 ^{0} C/µm. To obtain ±10% of this MTF (5.49 years and 6.7 years) with fixed current density and temperature, temperature gradient increases from 0.2 ^{0}C/µm to 0.211 ^{0}C/µm and decreases to 0.189 ^{0}C/µm respectively. Therefore, the accuracy of the temperature sensor gradient sensor also has to be very high.

If the temperature gradient is measured by taking the difference of two temperatures that are 10 µm apart, the temperature difference must be accurate to 0.11^{0}C to maintain ±10% accuracy in the MTF. Practically, some of the measurement error budget should be allocated to the temperature sensor and some to the temperature gradient sensor.

Therefore, to maintain the ±10% accuracy in the MTF, if the temperature accuracy is increased to ±1.2^{0}C, the temperature gradient measurement could be reduced to 0.003^{0}C/µm and the corresponding temperature difference accuracy to 0.03^{0}C. At this stage, whether it is ultimately practical to maintain accuracy of a target MTF that is within ±10% of the target MTF is not clear. Unless some major breakthrough occurs in the design of temperature sensors, a single point temperature calibration during production testing will be necessary. The overall accuracy of the calibrated temperature sensor will be the sum of the accuracy of the calibration temperature and the accuracy of the temperature sensor itself. In existing production test flows, it is difficult to measure the calibration temperature at a sensor point on the silicon wafer to much better than ±1^{0}C. This places a lower bound on the accuracy of the temperature sensor. So, if the temperature sensor accuracy requirement is ±1.2^{0}C, the accuracy of the temperature sensor circuit itself must be at the ±0.2^{0}C level which is achievable. Since the gradient sensor depends on temperature difference rather than an absolute temperature, reasonable performance of a temperature gradient sensor may be achievable without calibration.

المنارة للاستشارات

www.manaraa.com

CHAPTER 5 – CONCLUSION

Silicon wears out under normal stress. Existing approaches to reliability modeling that are "silent" about the reliability issue and that ignore the actual time-dependent stress come at the expense of dramatic degradation in the tradeoffs between performance and reliability in integrated circuits that manufactured today. In this work a time-dependent stress model has been introduced for predicting reliability of electromigration-sensitive metal interconnects. The stress is defined by a single parameter μ which is a function of temperature, T, current density, J and temperature gradient, ΔT. By varying T, J and ΔT, a set of different stress values were generated to predict the median time to failure (MTF) of the metal interconnect.

It is observed that inclusion of the time-dependent stress in the prediction of reliability can dramatically improve the accuracy of lifetime predictions. Simulation results showed over a 300% improvement in lifetime prediction accuracy can be achieved by including the time-varying stress in the reliability modeling when considering even a modest time-varying stress situation. The results would be even more dramatic under many realistic use conditions. If real-time stress history is monitored throughout the life of a part and used to establish dynamic stress guard bands, significant improvements in performance will often be possible without compromising target reliability of a system. It was also shown that to achieve ±10% accuracy of the MTF under constant stress, the power/thermal management circuit that uses temperature measurements to trigger throttling requires accuracy of the temperature sensor at the $\pm 1.6^{0}$C level.

It was also observed that thermal gradients due to joule heating or due to other factors contribute to stress and in the presence of electrical and thermal stress, thermal gradients significantly contribute to degradation in reliability as well even under constant stress conditions.

المنارة للاستشارات
www.manaraa.com

The enhanced reliability degradation due to thermal gradients in the presence of electrical and thermal stress is likely to get much worse as power density increases in next-generation systems. By incorporating the output of a number of strategically placed thermal and thermal gradient sensors in the power/thermal management algorithm, significant improvements in reliability can be achieved while still meeting target reliability goals. Good accuracy on the temperature sensors and the temperature gradient sensors is needed if tight MTF goals are to be met. With increases in the number of cores in many microcontroller systems, and with projections for increasing the total power dissipation on processors in the next few years while maintaining approximately the same die area, much larger thermal gradients can be expected and these thermal gradients will likely play increasingly important roles in the reliability of interconnects.

المنارة للاستشارات

www.manaraa.com

REFERENCES

[1] Lucile Arnauda et. al, “Microstructure and electromigration in copper damascene lines”, Microelectronics Reliability, pp 77-86, 2000

[2] Black, J.R., “Mass Transport of Aluminum by Momentum Exchange with Conducting Electrons”, Reliability Physics Symposium, pp 148-159, 1967

[3] Black, J.R., “Electromigration Failure Modes in Aluminum Metallization for Semiconductor Devices”, Proceedings of the IEEE, pp 1587-1594, 1969

[4] Takenao Nemoto, Tutomu Murakawa and A. Toshimitsu Yokobori, “Numerical Analysis for Electromigration of Cu Atom”, Journal of Materials Transactions, pp 2513 - 2517, 2007

[5] Syed M. Alam et. al, “Electromigration Reliability Comparison of Cu and Al Interconnects” Proceedings of the Sixth International Symposium on Quality Electronic Design (ISQED), 2005

[6] Jung Woo Pyun, “Electromigration behavior of 60 nm dual damascene Cu interconnects”, Journal of Applied Physics, 2007

[7] R. G. Filippi et. al, “The Effect of a Threshold Failure Time and Bimodal Behavior on the Electromigration Lifetime of Copper Interconnects”, IEEE CFP09RPS-CDR 47th Annual International Reliability, Physics Symposium, Montreal, 2009

[8] Vincent M. Dwyer, “Electromigration Behavior Under a Unidirectional Time-Dependent Stress”, IEEE Transactions on electron devices, pp 877-882, 1996

[9] Baozhen Li et. al,“Minimum Void Size and 3-Parameter Lognormal Distribution for EM Failures in CU Interconnects, IEEE 44th Annual International Reliability Physics Symposium, San Jose, 2006

[10] H.V Nguyen et. al, “Effect of Thermal Gradients on the Electromigration lifetime in Power Electronics”, IEEE annual international reliability physics symposium, 2004

[11] Jeng-Liang Tsai et. al, “Temperature-Aware Placement for SOCs”, Proceedings of the IEEE August 2006

[12] P.E. Gronowski, W.J. Bowhill, R.P. Preston, M.K. Gowan, and R.L. Allmon, “High performance microprocessor design,” IEEE J. Solid State Circuits, pp. 676-686, 1998

[13] Q. Wu, Q. Qiu, and M. Pedram, “Dynamic power management of complex systems using generalized stochastic Petri nets,” Proc. Design Automation Conf, pp. 352-356, June 2000

[14] S. Im and K. Banerjee, “Full chip thermal analysis of planar (2-D) and vertically integrated (3-D) high performance ICs,” Tech. Digest IEDM, pp. 727-730, 2000

المنارة للاستشارات
www.manaraa.com

[15] K. Banerjee A. Mehrotra, A. Sangiovanni-Vincentelli, and C. Hu, "On thermal effects in deep sub-micron VLSI interconnects," Proc. Design Automation Conf, pp. 885-891,1999

[16] A. H. Ajami et. al, "Analysis of non-Uniform temperature-Dependent interconnect performance in high-performance", Design Automation Conference proceedings, 2001

[17] Blish, R. and Durrant, N., "Semiconductor Device Reliability Failure Models, Technology Transfer # 00053955A-XFR, International SEMATECH, 2000

[18] Meeker, W. and Escobar, L., "Statistical Methods for Reliability Data", Wiley, 1998.

[19] Alam. S et. al," Electromigration Reliability Comparison of Cu and Al Interconnects", IEEE ISQED, 2005.

[20] Shor. J et. al, "Ratiometirc BJT based Thermal Sensor in 32 nm and 22 nm Technologies", pp 210-211, ISSCC, 2012

[21] Lloyd, J.R., "Electromigration for Designers", Simplex Solutions White Paper

[22] http://oldwww.ma.man.ac.uk/~mkt/334%20Reliability/Notes08/RelS1.pdf

المنارة للاستشارات

www.manaraa.com

PUBLICATIONS

1. Srijita Patra, Degang Chen, Randy Geiger, “Reliability Modeling of Metal Interconnects with Time -Dependent Electrical and Thermal Stress”, pp 514-517, International Midwest Symposium on Circuits and Systems (MWSCAS) August, 2012.

2. Srijita Patra, Degang Chen, Randy Geiger, “Reliability Degradation with Electrical, Thermal and Thermal Gradient Stress in Metal Interconnects”, pp 1063-1066, IEEE International Symposium on Circuits and Systems (ISCAS) May, 2013.

www.manaraa.com